

# Directional Wavelet Bases Construction on Dyadic Quincunx Lattice

Rujie Yin, Ingrid Daubechies

April 5, 2016

## *Abstract*

We construct directional wavelet systems that have the same direction selectivity as shearlets in the first frequency dyadic ring and non-uniform directional wavelet filterbanks(nuDFB). In particular, dilated quincunx downsampling is used to construct orthonormal and bi-orthogonal bases and standard dyadic downsampling for low-redundancy frames. We prove that the support of orthonormal and bi-orthogonal wavelets is discontinuous in the frequency domain, which can be avoided in frames of redundancy as low as 2. These are the first step towards the construction of efficient shearlet systems.

## 1 Introduction

In image compression and analysis, 2D tensor wavelet schemes are widely used. Despite the time-frequency localization inherited from 1D wavelet, 2D tensor wavelets suffers from poor orientation selectivity: only horizontal or vertical edges are well represented by tensor wavelets. To obtain better representation of 2D images, several directional wavelet schemes have been proposed and applied to image processing, including directional wavelet filterbanks(DFB), contourlet, curvelet, shearlet and dual-tree wavelet.

Conventional DFB [1] divides the frequency domain into eight equi-angular pairs of triangles and it is critically downsampled (maximally decimated) and perfect reconstruction (PR), but without multi-resolution structure. A non-uniform DFB(nuDFB) is introduced in [2] where the high frequency ring is divided into six equi-angular pairs of trapezoids and the central low frequency square is kept for division in the next level of decomposition. The nuDFB is solved directly by optimization which provides a non-unique near orthogonal or bi-orthogonal solution depending on the initialization. Contourlets [3] combine the Laplacian pyramid scheme with DFB which has PR but with redundancy 4/3 inherited from the Laplacian pyramid. Shearlet [4, 5] and curvelet [6] systems construct a multi-resolution partition of the frequency domain by applying shear or rotation operators to a generator function in each level. Depending on the generator function and the number of directions, available shearlet and curvelet

implementations have redundancy at least 4; moreover, the factor may grow with the decomposition level. Dual-tree wavelets [7] are linear combinations of 2D tensor wavelets (corresponding to multi-resolution systems) that constitute an approximate Hilbert transform pair.

None of these schemes is PR, critically downsampled and regularized (localized in both time and frequency) with multi-resolution structure. In the framework of nuDFB ([2]), it is shown by Durand [8] that it's impossible to construct orthonormal filters localized in frequency without discontinuity in their frequency support, or equivalently regularized filters without aliasing. His construction of directional filters using compositions of 2-band filters associated to quincunx lattice, similar to that of uniform DFB in [2] and as pointed out in [2] the overall composed filters are not alias-free.

In this paper, we consider multi-resolution directional wavelets corresponding to the same partition of frequency domain as nuDFB and build a framework to analyze the equivalent conditions of PR for critically downsampled and more generally redundant schemes. In our previous work [9], we show that in multi-resolution analysis(MRA), PR is equivalent to an identity condition and shift-cancellation condition closely related to the frequency support of filters and their downsampling scheme. Based on these two conditions, we derive Durand's discontinuity result of orthonormal schemes and a relaxation of orthonormal schemes to frame with redundancy 2 that resolves the regularity limitation. A regularized directional wavelet scheme of redundancy 2 that satisfies the identity condition and the relaxed shift-cancellation condition, is constructed directly by smoothing the Fourier transform of the corresponding wavelet. We extend our previous work here and show that the same irregularity in orthonormal schemes exists in bi-orthogonal schemes. Our analysis of bi-orthogonal schemes is based on a numerical algorithm introduced by Cohen et al in [10] for constructing compactly supported symmetric wavelet bases on hexagonal lattice. We extend and adapt this algorithm to our bi-orthogonal framework.

The paper is organized as follows, in section 2, we set up our framework of a dyadic MRA with dilated quincunx downsampling. In section 3, we review the irregularity of orthonormal schemes in [9]. In particular, we derive two conditions, *identity summation* and *shift cancellation*, equivalent to perfect reconstruction in this MRA with critical downsampling. These lead to the classification of *regular/singular* boundaries of the frequency partition and a *relaxed shift-cancellation* condition for low-redundancy MRA frame allows better regularity of the directional wavelets. In section 6, we show the irregularity for bi-orthogonal schemes. We first review the wavelet construction algorithm in [10] which solves linear systems generated from regularity constraints. Next, we extend the algorithm to our framework and show that the resulting linear system doesn't have feasible solution satisfying all regularity constraints, especially continuity of Fourier transforms of wavelet filters. Finally, we conclude our results and discuss future work in section 9.

## 2 Framework Setup

We summarize 2D-MRA systems and the relation between frequency domain partition and sub-lattice of  $\mathbb{Z}^2$  with critical downsampling following [9].

### 2.1 Notation

Throughout this paper, we use lower case normal font for function, normal font for scalar, upper case bold font for matrix, lower case bold font for vector and upper case normal font for frequency domain.

### 2.2 Multi-resolution analysis and sub-lattice sampling

In an MRA, given a scaling function  $\phi \in L^2(\mathbb{R}^2)$ , s.t.  $\|\phi\|_2 = 1$ , the base approximation space is defined as  $V_0 = \overline{\text{span}\{\phi_{0,\mathbf{k}}\}_{\mathbf{k} \in \mathbb{Z}^2}}$ , where  $\phi_{0,\mathbf{k}} = \phi(\mathbf{x} - \mathbf{k})$ . If  $\langle \phi_{0,\mathbf{k}}, \phi_{0,\mathbf{k}'} \rangle = \delta_{\mathbf{k},\mathbf{k}'}$ , then  $\{\phi_{0,\mathbf{k}}\}$  is an orthonormal basis of  $V_0$ . In addition,  $\phi$  is associated with a scaling matrix  $\mathbf{D} \in \mathbb{Z}^{2 \times 2}$ , s.t. the dilated scaling function  $\phi_1(\mathbf{x}) = |\mathbf{D}|^{-1/2} \phi(\mathbf{D}^{-1}\mathbf{x})$  is a linear combination of  $\phi_{0,\mathbf{k}}$ . Equivalently,  $\exists m_0(\boldsymbol{\omega}) = m_0(\omega_1, \omega_2)$ ,  $2\pi$ -periodic in  $\omega_1, \omega_2$ , s.t. in the frequency domain

$$\hat{\phi}(\mathbf{D}^T \boldsymbol{\omega}) = m_0(\boldsymbol{\omega}) \hat{\phi}(\boldsymbol{\omega}). \quad (1)$$

Hence

$$\hat{\phi}(\boldsymbol{\omega}) = (2\pi)^{-1} \prod_{k=1}^{\infty} m_0(\mathbf{D}^{-k} \boldsymbol{\omega}). \quad (2)$$

Define the nested approximation spaces  $V_l = \overline{\text{span}\{\phi(\mathbf{D}^{-l}\mathbf{x} - \mathbf{k}); \mathbf{k} \in \mathbb{Z}^2\}}$ ,  $l \in \mathbb{Z}$  and  $W_l$  as the orthogonal complement of  $V_l$  with respect to  $V_{l-1}$  in MRA. Suppose there are  $J$  wavelet functions  $\psi^j \in L^2(\mathbb{R}^2)$ ,  $1 \leq j \leq J$ , and  $\mathbf{Q} \in \mathbb{Z}^{2 \times 2}$ , s.t.

$$W_1 = \bigcup_{j=1}^J W_1^j = \bigcup_{j=1}^J \overline{\text{span}\{\psi_{1,\mathbf{k}}^j; \mathbf{k} \in \mathbf{Q}\mathbb{Z}^2\}} = \bigcup_{j=1}^J \overline{\text{span}\{\psi^j(\mathbf{D}^{-1}\mathbf{x} - \mathbf{k}); \mathbf{k} \in \mathbf{Q}\mathbb{Z}^2\}}.$$

An  $L$ -level multi-resolution system with base space  $V_0$  is then spanned by

$$\{\phi_{L,\mathbf{k}}, \psi_{l,\mathbf{k}'}^j, 1 \leq l \leq L, \mathbf{k} \in \mathbb{Z}^2, \mathbf{k}' \in \mathbf{Q}\mathbb{Z}^2, 1 \leq j \leq J\}. \quad (3)$$

In particular, we set  $\mathbf{D} = \mathbf{D}_2 \doteq \begin{pmatrix} 2 & 0 \\ 0 & 2 \end{pmatrix}$  and  $\mathbf{Q} := \begin{pmatrix} 1 & 1 \\ -1 & 1 \end{pmatrix}$ . As  $W_1 \subset V_0$ , each rescaled wavelet  $\psi^j(\mathbf{D}^{-1}\cdot)$  is also a linear combination of  $\phi_{0,\mathbf{k}}$ , so that  $\exists m_j$  analogous to  $m_0$  satisfying

$$\hat{\psi}^j(\mathbf{D}^T \boldsymbol{\omega}) = m_j(\boldsymbol{\omega}) \hat{\phi}(\boldsymbol{\omega}), \quad 1 \leq j \leq J. \quad (4)$$

In this construction of MRA, the corresponding subsampling matrix of  $\phi_{1,\mathbf{k}}$  is  $\mathbf{D}$  and that of  $\psi_{1,\mathbf{k}}^j$  is  $\mathbf{QD}$ , the dilated quincunx subsample (see the right panel in Fig.1), as in [8].

### 2.3 Frequency domain partition and critical downsampling

Consider the canonical frequency square,  $S_0 = [-\pi, \pi) \times [-\pi, \pi)$  associated with lattice  $\mathcal{L} = \mathbb{Z}^2$ . If  $C_j$  are the main support of  $m_j$ ,  $0 \leq j \leq J$ , then due to

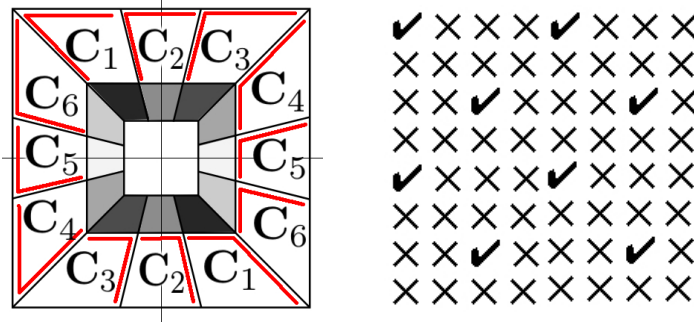


Figure 1: Left: partition of  $S_0$  and boundary assignment of  $C_j$ ,  $j = 1, \dots, 6$  (each  $C_j$  has boundaries indicated by red line segments), Right: dilated quincunx sub-lattice.

(1) and (4) they form a partition of  $S_0$ . To build an orthonormal basis with good directional selectivity, we choose the partition of  $S_0$  to be that of the least redundant shearlet system, see Fig.1 left, which is also Example B in [8]. In this partition,  $S_0$  is divided into a central square  $C_0 = S_1 := \begin{pmatrix} 2 & 0 \\ 0 & 2 \end{pmatrix}^{-1} S_0$  and a ring: the ring is further cut into six pairs of directional trapezoids  $C_j$ 's by lines passing through the origin with slopes  $\pm 1, \pm 3$  and  $\pm \frac{1}{3}$ . The central square  $S_1$  can be further partitioned in the same way to obtain a two-level multi-resolution system, as shown in Fig.1.

Here  $J = 6$  and  $|\mathbf{D}|^{-1} + J|\mathbf{QD}|^{-1} = 1/4 + 6/(2 \cdot 4) = 1$ , hence the corresponding MRA generated by (3) achieves critical downsampling([8]). Furthermore, let  $\pi_0 = (0, 0), \pi_1 = (\pi/2, \pi/2), \pi_2 = (\pi, 0), \pi_3 = (-\pi/2, \pi/2), \pi_4 = (0, \pi), \pi_5 = (\pi/2, -\pi/2), \pi_6 = (\pi, \pi), \pi_7 = (-\pi/2, -\pi/2)$ , then each piece  $C_j$  together with its shifts form a tiling of  $S_0$ , i.e.

$$S_0 = \bigcup_{\pi \in \Gamma_0} (C_j + \pi) = \bigcup_{\pi \in \Gamma_1} (C_0 + \pi), \quad j = 1, \dots, 6$$

where  $\Gamma_0 = \{\pi_i, i = 0, 2, 4, 6\}$  and  $\Gamma_1 = \{\pi_i, i = 0, \dots, 7\}$ .

### 3 Orthonormal Bases

In this section, we consider orthonormal bases with  $m$ -functions defined in (1) and (4) whose supports mainly corresponding to the partition of  $S_0$  in Fig.1.

The construction of (3) reduces to design  $m_0$  in (1) and  $m_j, j = 1, \dots, 6$  in (4). We begin with examining the conditions on  $m$ -functions such that the system (3) is perfect reconstruction (PR) or equivalently a Parseval frame in MRA.

#### 3.1 Identity summation and shift cancellation

In MRA, (3) is PR if  $\forall f \in L_2(\mathbb{R}^2)$ ,

$$\sum_k \langle f, \phi_{0,k} \rangle \phi_{0,k} = \sum_k \langle f, \phi_{1,k} \rangle \phi_{1,k} + \sum_j \sum_k \langle f, \psi_{1,k}^j \rangle \psi_{1,k}^j. \quad (5)$$

Using (1) and (4) together with the admissibility of the frequency partition, this condition on  $\phi$  and  $\psi^j$ 's yields:

**Theorem 1.** *The perfect reconstruction condition holds for (3) iff the following two conditions hold*

$$|m_0(\omega)|^2 + \sum_{j=1}^6 |m_j(\omega)|^2 = 1 \quad (6)$$

$$\begin{cases} \sum_{j=0}^6 m_j(\omega) \overline{m_j(\omega + \pi)} = 0, & \pi \in \Gamma_0 \setminus \{\mathbf{0}\} \\ \sum_{j=1}^6 m_j(\omega) \overline{m_j(\omega + \pi)} = 0, & \pi \in \Gamma_1 \setminus \Gamma_0 \end{cases} \quad (7)$$

Theorem 1 is a corollary of Prop. 1 and Prop. 2 in [8]. We give an alternate proof in Appendix A. In Theorem 1, Eq. (6) is the *identity summation* condition, guaranteeing conservation of  $l_2$  energy; Eq. (7) is the *shift cancellation* condition such that aliasing is canceled correctly in reconstruction.

### 3.2 Extra condition for basis

By Theorem 1, the system (3) is a Parseval frame ; for it to be an orthonormal basis,  $\{\phi_{\mathbf{k}}\}_{\mathbf{k} \in \mathbb{Z}^2}$  need to be an orthonormal basis. Because  $\phi$  is determined by  $m_0$  in (2) (like in 1D MRA), we can find a necessary and sufficient condition on  $m_0$  such that (3) is an orthonormal basis. The following theorem is a 2D generalization of Cohen's 1D theorem in [11].

**Theorem 2.** *Assume that  $m_0$  is a trigonometric polynomial with  $m_0(0) = 1$ , and define  $\hat{\phi}(\omega)$  as in (2).*

*If  $\phi(\cdot - \mathbf{k}), \mathbf{k} \in \mathbb{Z}^2$  are orthonormal, then  $\exists K$  containing a neighborhood of 0, s.t.  $\forall \omega \in S_0, \omega + 2\pi \mathbf{n} \in K$  for some  $\mathbf{n} \in \mathbb{Z}^2$ , and  $\inf_{k>0, \omega \in K} |m_0(\mathbf{D}_2^{-k} \omega)| > 0$ . Further, if  $\sum_{\pi \in \Gamma_0} |m_0(\omega + \pi)|^2 = 1$ , then the inverse is true.*

Theorem 2 can be proved similarly to Cohen's theorem ([11]). Below, we construct  $m$ -functions imposing only (6) and (7) and then check if the resulting Parseval frame is an orthonormal basis by applying Theorem 2 to  $m_0$ .

## 4 $m$ -function Design and Boundary Regularity

In this section, we define Shannon-type directional orthonormal basis same as in [8] and [2]. Then, we apply direct smoothing to its  $m$ -functions to improve spatial localization, this leads to a critical analysis of the boundary regularity of  $S_1$  and the  $C_j$ 's.

### 4.1 Shannon-type wavelets and smoothing

If each  $m_j$  is an indicator function of a piece in the partition of  $S_0$ , i.e.  $m_0 = \mathbb{1}_{S_1}$ ,  $m_j = \mathbb{1}_{C_j}$ ,  $1 \leq j \leq 6$ , and we use the boundary assignment of  $C_j$  in the left of Fig.1, then the identity summation follows from the frequency partition, and

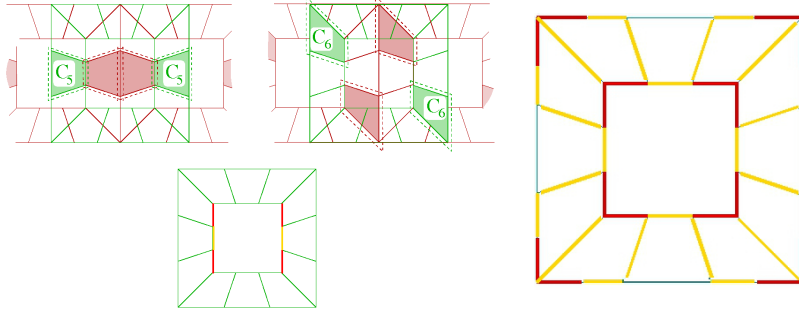


Figure 2: *Left top*: the supports of  $m_j$  (green) and  $m_j(\cdot + \pi_2)$  (red) for  $j = 5, 6$  after smoothing, overlap on the vertical boundary at  $\omega_1 = \pm\pi/2$  of  $C_5$  (green) and its shift (red) by  $\pi_2 = (\pi, 0)$ . Note that two copies of shifted  $S_0$  (red) overlap the un-shifted  $S_0$  (green) due to the  $(2\pi, 2\pi)$  periodicity of  $m_j$ . Only  $m_0$  and  $m_5$  have overlapping smoothed boundaries by  $\pi_2$ .

*Left bottom*: intersection of  $\mathcal{B}(0, \pi_2)$  and  $\mathcal{B}(5, \pi_2)$  in yellow and  $\mathcal{C}(0, \pi_2) = \mathcal{B}(0, \pi_2) \setminus \mathcal{B}(5, \pi_2)$  in red. Smoothing  $m_0$  in the red (singular) region is impossible without violating (7).

*Right*: boundary classification, singular (red) and regular (yellow) after similar arguments for all shifts  $\pi_i$ .

the shift cancellation holds automatically due to  $m_j(\omega)\overline{m_j(\omega + \pi_i)} \equiv 0, \forall j, i \neq 0$ . The Shannon-type wavelets generated from these  $m$ -functions form an orthonormal basis.

However, because of the discontinuity of  $m_j$  across the boundary of its support, the corresponding wavelet has slow decay in the time domain. In order to improve their spatial localization,  $m_j$  need to be regularized.

We take a different regularization approach from Durand's [8], where three regular quincunx filter banks are constructed and then composed to obtain the desired regular quincunx dyadic filter banks. Here, we smooth the discontinuous boundaries of  $m$ -functions directly. As shown in Proposition 3 in [8], it is not possible to smooth all the discontinuous boundaries if  $m_j$  satisfy the perfect reconstruction condition. Yet, we shall see that partial direct smoothing on regular boundaries is still possible.

## 4.2 Boundary classification

After smoothing the  $m_j$ 's, the shift cancellation (7) may fail to hold as  $\text{supp}(m_j)$  and  $(\text{supp}(m_j) - \pi)$  may overlap near the smoothed boundaries, see Fig. 2, illustrating  $m_5(\omega)\overline{m_5(\omega + \pi_2)} \neq 0$ . For simplicity, we introduce the following notations: let  $\mathcal{B}(j, \pi) = \text{supp}(m_j) \cap (\text{supp}(m_j) - \pi)$  be the support of  $m_j(\omega)\overline{m_j(\omega + \pi)}$  associated to  $m_j$  and shift  $\pi$ ; let  $\mathcal{C}(j, \pi) = \mathcal{B}(j, \pi) \setminus \bigcup_{j' \neq j} \mathcal{B}(j', \pi)$ .

**Lemma 1.** *Shift cancellation (7) can hold for shift  $\pi \in \Gamma_0 \setminus \{0\}$ , only if  $\mathcal{C}(j, \pi) = \emptyset, \forall 0 \leq j \leq 6$ ; it can hold for shift  $\pi \in \Gamma_1 \setminus \Gamma_0$ , only if  $\mathcal{C}(j, \pi) =$*

$\emptyset, \forall 1 \leq j \leq 6$ .

*Proof.* Observe that, on  $\mathcal{C}(j, \pi)$ ,  $m_j(\omega)\overline{m_j(\omega + \pi)} \neq 0$  but  $m_{j'}(\omega)\overline{m_{j'}(\omega + \pi)} \equiv 0, \forall j' \neq j$ , hence (7) doesn't hold.  $\square$

Therefore, boundaries that after smoothing make  $\mathcal{C}(j, \pi)$  non-empty are called *singular*; the rest are *regular*. We next provide an explicit boundary classification method:

**Proposition 1.**  $\forall 1 \leq j \leq 6$ , let  $\text{supp}(m_j) = \overline{C_j}$ , then the boundary of  $C_j$  is  $\partial C_j = \bigcup_{i \neq 0} \mathcal{B}(j, \pi_i)$ . The set of singular boundaries of  $\partial C_j$  is  $\bigcup_{i \neq 0} \mathcal{C}(j, \pi_i)$ , whereas its complement set is the regular boundary set.

*Proof.* Since  $\bigcup_i (C_j + \pi_i) = S_0$ ,  $\partial C_j \subset \bigcup_{i \neq 0} (\overline{C_j} + \pi_i)$ . Therefore,  $\partial C_j \subset \bigcup_{i \neq 0} \mathcal{B}(j, \pi_i)$ . On the other hand,  $\mathcal{B}(j, \pi_i) \subset \partial C_j, \forall i \neq 0$ , hence the union of them is a subset of  $\partial C_j$ . It follows that  $\mathcal{B}(j, \pi_i)$  form a partition of the boundary  $\partial C_j$ . The partition of  $\partial C_j$  into singular and regular boundaries follows from Lemma 1.  $\square$

The case of  $\partial S_1$  is similar where  $\mathcal{B}(0, \pi), \pi \in \Gamma_0 \setminus \{0\}$  are considered. We use the notation  $\mathcal{B}_s(j, \pi), \mathcal{C}_s(j, \pi)$  for the special case  $\text{supp}(m_j) = \overline{C_j}$  hereafter. The boundary classification based on Proposition 1 is shown in the right of Fig. 2, where the boundaries on the four corners of both  $S_0$  and  $S_1$  are singular: smoothing is then not allowed there.

**Proposition 2.** Let  $\mathcal{C} = \mathcal{C}_s(j_1, \pi_{i_1}) \cap \mathcal{C}_s(j_2, \pi_{i_2})$ , if  $m_{j_1}, m_{j_2}$  satisfy (6), (7), then  $|m_{j_1}| = \mathbb{1}_{\mathcal{C}_{j_1}}, |m_{j_2}| = \mathbb{1}_{\mathcal{C}_{j_2}}$  on  $\mathcal{C}$ .

*Proof.* Suppose the common singular boundary  $\mathcal{C}$  is non-empty and observe that  $\mathcal{C} \subset (C_{j_1}) \cap (C_{j_2})$ . Since  $m_{j_1}$  cannot be smoothed on  $\mathcal{C}_s(j_1, \pi_{i_1})$ ,  $|m_{j_1}| = 0$  on  $\mathcal{C}_s(j_1, \pi_{i_1}) \setminus \mathcal{C}_{j_1}$ , and (6) implies that  $|m_{j_2}| = 1$  there, or equivalently  $|m_{j_2}| = \mathbb{1}_{\mathcal{C}_{j_2}}$  on  $\mathcal{C}$ . Similarly,  $|m_{j_1}| = \mathbb{1}_{\mathcal{C}_{j_1}}$  on  $\mathcal{C}$ .  $\square$

Prop. 2 shows that if  $m_j$  and  $m_{j'}$  have common singular boundaries, then both will have a discontinuity across those boundaries. For example,  $\mathcal{C}_s(0, (\pi, 0)) \cap \mathcal{C}_s(4, (\pi/2, \pi/2)) = (\pi/2, (\pi/6, \pi/2))$ , hence  $m_0$  and  $m_4$  both are discontinuous at  $(\pi/2, (\pi/6, \pi/2))$ . All the singular boundaries related to (3) are such "double" singular boundaries.

### 4.3 Pairwise smoothing of regular boundary

The regular boundaries of both  $C_{j_1}$  and  $C_{j_2}$  with adjacent supports consist of  $\mathcal{B}_s(j_1, \pi) \cap \mathcal{B}_s(j_2, \pi)$ , which we denote by the triple  $(j_1, j_2, \pi)$ . The following proposition shows that the regular boundaries  $(j_1, j_2, \pi)$  can be paired according to shift pairs  $(\pi, -\pi)$ , and the boundaries must be smoothed pairwise within their  $\epsilon$ -neighborhood,  $\mathcal{B}_\epsilon(j_1, j_2, \pi)$  and  $\mathcal{B}_\epsilon(j_1, j_2, -\pi)$ .

**Proposition 3.** Given  $(j_1, j_2, \pi) \neq \emptyset$ , then  $(j_1, j_2, -\pi) \neq \emptyset$ . In addition, let  $\mathcal{B} = \mathcal{B}_\epsilon(j_1, j_2, \pi) \cup \mathcal{B}_\epsilon(j_1, j_2, -\pi)$ . Then the identity summation and shift cancellation conditions hold if

$$(i) \ m_j = \mathbb{1}_{C_j}, \quad \text{on } S_0, \ j \neq j_1, j_2$$

(ii)  $m_{j_1} = \mathbb{1}_{C_{j_1}}, m_{j_2} = \mathbb{1}_{C_{j_2}}, \quad \text{on } \mathcal{B}^c$

and on  $\mathcal{B}$  the following hold

(iii)  $|m_{j_1}|^2 + |m_{j_2}|^2 = 1,$

(iv)  $\sum_{j_1, j_2} m_j(\cdot) \overline{m_j(\cdot + \tilde{\pi})} = 0, \tilde{\pi} = \pm \pi$

*Proof.* We first show that  $(j_1, j_2, -\pi) \neq \emptyset$ . By definition,  $\mathcal{B}_s(j_1, \pi) = \text{supp}(m_{j_1}) \cap (\text{supp}(m_{j_1}) - \pi) = ((\text{supp}(m_{j_1}) + \pi) \cap \text{supp}(m_{j_1})) - \pi = \mathcal{B}_s(j_1, -\pi) - \pi$ . Rewrite  $(j_1, j_2, \pi)$  by  $\mathcal{B}_s(j_1, -\pi)$  and  $\mathcal{B}_s(j_2, -\pi)$ , we have  $(j_1, j_2, -\pi) = (j_1, j_2, \pi) + \pi$ , hence it's non-empty.

Because  $(j_1, j_2, \pm\pi) \subset (\partial C_{j_1} \cap \partial C_{j_2})$  and  $(\bigcup_j C_j) = S_0, (\bigcup_{j \neq j_1, j_2} C_j) \cap \mathcal{B} = \emptyset$ . Therefore, smoothing of  $m_{j_1}$  and  $m_{j_2}$  in  $\mathcal{B}$  doesn't impact the region where other  $m_j$ 's are supported.

We then show that the cancellation conditions (7) hold for all shifts. Condition (i) and (ii) imply that  $\mathcal{B}(j, \tilde{\pi}) = \emptyset, \forall j, \tilde{\pi} \neq \pm\pi$ , hence (7) hold for  $\tilde{\pi} \neq \pm\pi$ . (i) implies  $\mathcal{B}(j, \tilde{\pi}) = \emptyset, \forall j \neq j_1, j_2$ , so then (7) is equivalent to (iv). The identity summation (6) holds due to (i), (ii) and (iii).  $\square$ .

By Prop. 3 we can smooth some pairs of regular boundaries starting from the Shannon-type directional wavelets with the simplified conditions (iii), (iv) and (v); (i) and (ii) can be removed as long as the initial  $m_j$  satisfy (6) and (7) and every  $\omega \in S_0$  is not covered by more than two  $m$  functions. We can thus smooth regular boundaries pairwise, one by one.

The next proposition gives an explicit design of  $(m_{j_1}, m_{j_2})$  satisfying the simplified conditions (iii), (iv) in Proposition 3.

**Proposition 4.** *Let  $C \subset S_0$ , given  $m_{j_1}, m_{j_2} \neq 0$  continuous on  $C \cup (C + \pi)$ , satisfying the following conditions*

(i)  $\sum_{j_1, j_2} m_j(\omega) \overline{m_j(\omega + \pi)} = 0 \quad \text{on } C$

(ii)  $\sum_{j_1, j_2} |m_j(\omega)|^2 = 1 \quad \text{on } C \cup (C + \pi)$

(iii)  $m_{j_1}(\omega) m_{j_2}(\omega) = 0 \quad \text{on } \partial C ;$

then  $|m_{j_1}(\omega)| = |m_{j_2}(\omega + \pi)|, |m_{j_2}(\omega)| = |m_{j_1}(\omega + \pi)|.$

Furthermore, if  $m_j = e^{i\omega^T \boldsymbol{\eta}_j} m_j, \quad j = j_1, j_2, \text{ on } C, \text{ where } m_j \text{ is a real-valued function, } e^{i\pi^T(\boldsymbol{\eta}_{j_1} - \boldsymbol{\eta}_{j_2})} = -1, \text{ and}$

$m_{j_1}(\omega) = m_{j_2}(\omega - \pi), m_{j_2}(\omega) = m_{j_1}(\omega - \pi), \text{ on } C + \pi,$

then (i) holds.

*Proof.* To prove the necessary condition, note that (i) implies  $|m_{j_1}(\omega)|^2 |m_{j_1}(\omega + \pi)|^2 = |m_{j_2}(\omega)|^2 |m_{j_2}(\omega + \pi)|^2$ ; the condition then follows from (ii). For the sufficient construction, check by directly substituting the construction into (i).  $\square$

Proposition 4 breaks down the design of  $(m_{j_1}, m_{j_2})$  into a pair of real functions  $(m_{j_1}, m_{j_2})$  on  $\mathcal{B}_\epsilon(j_1, j_2, \pi)$  and two vectors  $\boldsymbol{\eta}_1, \boldsymbol{\eta}_2$ ; then  $(m_{j_1}, m_{j_2})$  on  $\mathcal{B}_\epsilon(j_1, j_2, -\pi)$  are automatically determined. The only constraint on  $(m_{j_1}, m_{j_2})$



for (ii) in Proposition 4 to hold is that on  $\mathcal{B}_\epsilon(j_1, j_2, \boldsymbol{\pi})$ ,  $\sum_{j_1, j_2} |m_j(\boldsymbol{\omega})|^2 = 1$ , which is easy to be satisfied. We may construct all local pairs of  $(m_{j_1}, m_{j_2})$  separately, and put together afterwards different pieces of each  $m_j$  located in different regular boundary neighborhoods  $\mathcal{B}_\epsilon(j, j', \boldsymbol{\pi})$ .

The next proposition gives one solution, easy to verify.

**Proposition 5.** *Applying Proposition 4 to all regular boundaries requires a set of phases  $\{\boldsymbol{\eta}_j\}_{j=0}^6$ , s.t.*

$$e^{i\boldsymbol{\nu}^T(\boldsymbol{\eta}_{j_1} - \boldsymbol{\eta}_{j_2})} = -1, \quad \forall (j_1, j_2, \boldsymbol{\pi}) \in \Delta,$$

$$\begin{aligned} \Delta = \{ & (0, 2, (0, \pi)), (0, 5, (\pi, 0)), (1, 3, (\pi, 0)), (4, 6, (0, \pi)), \\ & (1, 6, (\pi/2, 3\pi/2)), (2, 3, (\pi/2, 3\pi/2)), (4, 5, (\pi/2, 3\pi/2)), \\ & (3, 4, (\pi/2, \pi/2)), (1, 2, (\pi/2, \pi/2)), (5, 6, (\pi/2, \pi/2)) \} \end{aligned}$$

The following is a (non-unique) solution:

$$\begin{aligned} \boldsymbol{\eta}_0 &= (0, 0), \boldsymbol{\eta}_1 = (0, 0), \boldsymbol{\eta}_2 = (1, 1), \boldsymbol{\eta}_3 = (1, -1), \\ \boldsymbol{\eta}_4 &= (0, 2), \boldsymbol{\eta}_5 = (1, 1), \boldsymbol{\eta}_6 = (-1, 1). \end{aligned}$$

To summarize, Proposition 4 and 5 introduce the following regular boundary smoothing scheme for the  $m$  functions:

#### construction of orthonormal basis

1. First, set  $m_j = \mathbb{1}_{C_j}$ ; then smoothen these across a pair of regular boundaries  $(j_1, j_2, \pm\boldsymbol{\pi})$  following steps 2, 3.
2. On  $\mathcal{B}_\epsilon(j_1, j_2, \boldsymbol{\pi})$ ,  
design  $(m_{j_1}, m_{j_2})$ , s.t.  $\sum_{j_1, j_2} |m_j(\boldsymbol{\omega})|^2 = 1$ .
3. On  $\mathcal{B}_\epsilon(j_1, j_2, -\boldsymbol{\pi})$ ,  
let  $m_{j_1}(\boldsymbol{\omega}) = m_{j_2}(\boldsymbol{\omega} - \boldsymbol{\pi})$ ,  $m_{j_2}(\boldsymbol{\omega}) = m_{j_1}(\boldsymbol{\omega} - \boldsymbol{\pi})$
4. Repeat step 2 and 3 for all  $(j_1, j_2, \boldsymbol{\pi}) \in \Delta$ .
5.  $m_j(\boldsymbol{\omega}) = e^{i\boldsymbol{\omega}^T \boldsymbol{\eta}_j} m_j(\boldsymbol{\omega})$ , on  $S_0$ , with the  $\boldsymbol{\eta}_j$  of Prop. 5.

We apply this to smooth all the regular boundaries except those on the boundary of  $S_0$ . Near a regular boundary  $\mathcal{B}_\epsilon(j, j', \boldsymbol{\pi})$ , the discontinuity of  $|m_j|$  from 0 to 1 depends on  $m_j$ ; the contour of stop-band(pass-band) is the boundary of level set  $\{m_j(\boldsymbol{\omega}) = 0\} (\{m_j(\boldsymbol{\omega}) = 1\})$ . Fig. 3 shows our design of the stop-band/pass-band contours of regular boundaries  $(5, 6, (\frac{\pi}{2}, \frac{\pi}{2}))$  and  $(0, 5, (\pi, 0))$ . The contours intersect only at the vertices of  $C_5$ , e.g.  $\text{supp}(m_5) \cap \text{supp}(m_6) \cap \text{supp}(m_0)$  contains just one point. Moreover, we set  $m_5$  to be symmetric with respect to the origin near both regular boundaries.

The contours related to other regular boundaries are designed likewise to achieve the best symmetry; the corresponding wavelets are real. Fig.3 (right) shows the frequency support of directional wavelets generated by such design;

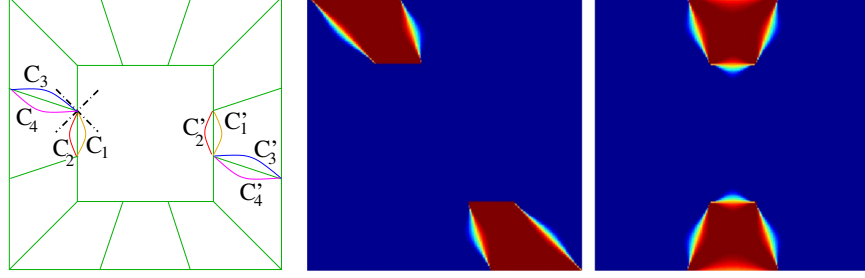


Figure 3: Left: contour design of  $\text{supp}(m_5)$ , Right: frequency support  $|\hat{\psi}^j|$

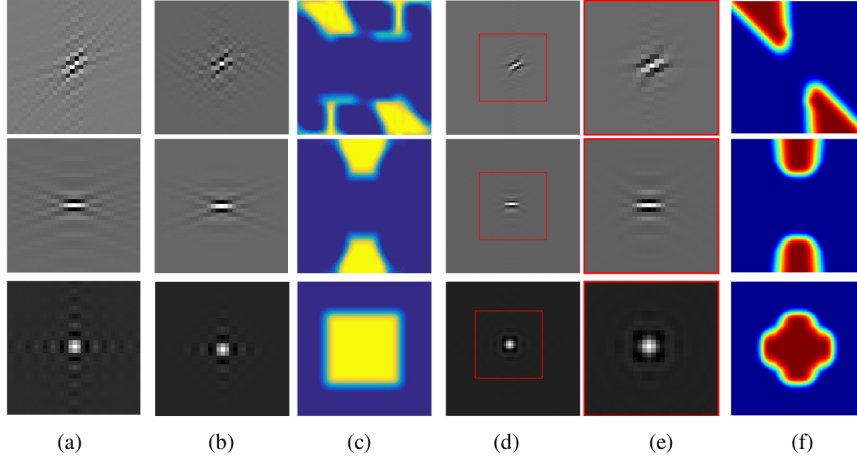


Figure 4: directional wavelets  $\psi^1, \psi^2$  and scaling function  $\phi$  in different constructions (a) our directional wavelet orthonormal basis, whose frequency support is shown in Fig. 3; (b) Durand's directional wavelet; (c)  $m$ -functions of wavelets in (b). (d) our directional wavelet frame; (e) zoom in on (d); (f)  $m$ -functions of wavelets in (d); Our basis construction in (a) has good frequency localization, but slowly decaying spatial oscillation; Durand's construction in (b) has good spatial localization but non-localized frequency support; our frame construction in (d) has both good frequency localization and spatial localization. Note that plots (a),(b),(e) are at the same resolution.

Fig.4(a) shows the wavelets and scaling function in space domain. One easily checks (using Theorem 2) that this is an orthonormal basis.

Although the wavelets orient in six directions, they are not very well localized spatially, due to the singular boundaries on the corners of the low-frequency square  $S_1$ , where the discontinuity in the frequency domain is inevitable. The lack of smoothness at the vertices of  $m_2$  and  $m_5$  could possibly be avoided by using a more delicate (but more complicated) design around the vertices  $(\pm \frac{\pi}{2}, \pm \frac{\pi}{6})$  allowing triple overlapping of  $m$ -functions.

Allowing a bit of redundancy (abandoning critical downsampling), we show

next how to construct a frame with low redundancy that has much better spatial localization.

## 5 Low-redundancy frame construction

Consider the  $L$ -level directional wavelet MRA system

$$\{\phi_{L,\mathbf{k}}, \psi_{l,\mathbf{k}'}^j, 1 \leq l \leq L, \mathbf{k}, \mathbf{k}' \in \mathbb{Z}^2, 1 \leq j \leq J\}. \quad (8)$$

where  $\phi, \psi^j$  satisfy (1) and (4) as before. Instead of taking the dilated quincunx subsampling of directional wavelet coefficients of (3), a dyadic subsampling is taken instead. A 1-level MRA frame (8) has redundancy  $\frac{1}{|D|} + \frac{J}{|D|} = 1/4 + 6/4 = 7/4$ , and the redundancy for any  $L$ -level MRA frame doesn't exceed  $\frac{J/|D|}{1-1/|D|} = \frac{6/4}{1-1/4} = 2$ . We have now

**Theorem 3.** *The perfect reconstruction condition holds for (8) iff the following both hold*

$$|m_0(\omega)|^2 + \sum_{j=1}^6 |m_j(\omega)|^2 = 1 \quad (9)$$

$$\sum_{j=0}^6 m_j(\omega) \overline{m_j(\omega + \pi)} = 0, \quad \pi \in \Gamma_0 \setminus \{\mathbf{0}\} \quad (10)$$

Thmeorem 3 can be proved analogously to Thmeorem 1, with fewer shift cancellation constraints now. We can define *singular* boundaries as before, but only  $\{\mathcal{B}(j, \pi)\}_{\pi \in \Gamma_0 \setminus \{\mathbf{0}\}}$  need to be considered, which results in fewer singular boundaries  $\{\mathcal{C}_s(j, \pi)\}_{\pi \in \Gamma \setminus \{\mathbf{0}\}}$ ; and no "double" singular boundaries now.

This means that even though  $\text{supp}(m_0)$  still cannot be extended outside of the four corners of  $S_1$  due to  $\mathcal{C}_s(0, (\pi, 0))$  and  $\mathcal{C}_s(0, (0, \pi))$ ,  $m_1$  can penetrate into the inside of  $S_1$  because  $\mathcal{C}_s(1, (\pi/2, 3\pi/2))$  is not a singular boundary in (8). The same is true for  $m_3, m_4$  and  $m_6$ . This makes smoothing the boundaries of  $m_0$  inwards possible without violating (6), see Fig. 4(c). At the price of double redundancy, we obtain directional wavelets with much better spatial localization; see Fig. 4(d)(e): the discontinuities of a directional wavelets basis in the frequency domain around the singular boundaries can be removed in a low redundant directional wavelet tight frame.

Heretofore, we have considered two directional wavelet MRA systems (3) and (8) such that the directional wavelets characterize 2D signals in six equi-angled directions. The orthonormal basis we construct has better frequency localization than the one constructed by Durand in [8] (see Fig. 3 and 4(b)(c)), but has long tails in certain spatial directions, unavoidable because of "double" singular boundaries. By doubling the redundancy we obtain spatially well localized directional wavelets. Furthermore, these wavelets are well localized in the frequency domain such that  $\text{supp}(m_j)$  is convex and  $\exists \epsilon$  s.t.

$$\sup_{\omega' \in \text{supp}(m_j)} \inf_{\omega \in C_j} \|\omega' - \omega\| < \epsilon, \quad 0 \leq j \leq 6. \quad (11)$$

This desirable condition is hard to obtain by multi-directional filter bank assembly of several elementary filter banks.

In the next section, we analyze the more general case of directional bi-orthogonal filters constructed with respect to the same frequency partition.

## 6 Bi-orthogonal Bases

In this section, we analyze the bi-orthogonal bases  $\{\phi_{L,\mathbf{k}}, \tilde{\phi}_{L,\mathbf{k}}, \psi_{l,\mathbf{k}}, \tilde{\psi}_{l,\mathbf{k}}, 1 \leq l \leq L, \mathbf{k} \in \mathbb{Z}^2, 1 \leq j \leq J\}$ , where  $\phi, \psi$  satisfy (1) and (4), and  $\tilde{\phi}, \tilde{\psi}$  satisfy the same MRA,

$$\hat{\phi}(\mathbf{D}^T \boldsymbol{\omega}) = \widetilde{m_0}(\boldsymbol{\omega}) \hat{\phi}(\boldsymbol{\omega}), \quad \hat{\tilde{\phi}}(\mathbf{D}^T \boldsymbol{\omega}) = \widetilde{m_0}(\boldsymbol{\omega}) \hat{\tilde{\phi}}(\boldsymbol{\omega}).$$

For bi-orthogonal bases, we have the similar identity summation and shift cancellation condition to Theorem 1.

**Theorem 4.** *The perfect reconstruction iff the following two conditions hold*

$$m_0(\boldsymbol{\omega}) \widetilde{m_0}(\boldsymbol{\omega}) + \sum_{j=1}^6 m_j(\boldsymbol{\omega}) \widetilde{m_j}(\boldsymbol{\omega}) = 1 \quad (12)$$

$$\begin{cases} \sum_{j=0}^6 m_j(\boldsymbol{\omega}) \widetilde{m_j}(\boldsymbol{\omega} + \boldsymbol{\pi}) = 0, & \boldsymbol{\pi} \in \Gamma_0 \setminus \{\mathbf{0}\} \\ \sum_{j=1}^6 m_j(\boldsymbol{\omega}) \widetilde{m_j}(\boldsymbol{\omega} + \boldsymbol{\pi}) = 0, & \boldsymbol{\pi} \in \Gamma_1 \setminus \Gamma_0 \end{cases} \quad (13)$$

The conditions (12) and (13) can be combined into a linear system as follows,

$$\begin{bmatrix} \widetilde{m_0}(\boldsymbol{\omega}) & \widetilde{m_1}(\boldsymbol{\omega}) & \dots & \widetilde{m_6}(\boldsymbol{\omega}) \\ 0 & \widetilde{m_1}(\boldsymbol{\omega} + \boldsymbol{\pi}_1) & \dots & \widetilde{m_6}(\boldsymbol{\omega} + \boldsymbol{\pi}_1) \\ \widetilde{m_0}(\boldsymbol{\omega} + \boldsymbol{\pi}_2) & \widetilde{m_1}(\boldsymbol{\omega} + \boldsymbol{\pi}_2) & \dots & \widetilde{m_6}(\boldsymbol{\omega} + \boldsymbol{\pi}_2) \\ \vdots & \vdots & \vdots & \vdots \\ 0 & \widetilde{m_1}(\boldsymbol{\omega} + \boldsymbol{\pi}_7) & \dots & \widetilde{m_6}(\boldsymbol{\omega} + \boldsymbol{\pi}_7) \end{bmatrix} \begin{bmatrix} m_0(\boldsymbol{\omega}) \\ m_1(\boldsymbol{\omega}) \\ m_2(\boldsymbol{\omega}) \\ \vdots \\ m_6(\boldsymbol{\omega}) \end{bmatrix} = \begin{bmatrix} 1 \\ 0 \\ 0 \\ \vdots \\ 0 \end{bmatrix} \quad (14)$$

In addition, the orthogonal condition on  $m_j, \widetilde{m_j}$  is an analogue of Theorem 2.

**Theorem 5.** *Assume that  $m_0, \widetilde{m_0}$  are trigonometric polynomials with  $m_0(0) = \widetilde{m_0}(0) = 1$ , which generate  $\phi, \tilde{\phi}$  respectively.*

*If  $\phi(\cdot - \mathbf{k}), \tilde{\phi}(\cdot - \mathbf{k}) \mathbf{k} \in \mathbb{Z}^2$  are bi-orthogonal, then  $\exists K$  containing a neighborhood of  $\mathbf{0}$ , s.t.  $\forall \boldsymbol{\omega} \in S_0, \boldsymbol{\omega} + 2\pi \mathbf{n} \in K$  for some  $\mathbf{n} \in \mathbb{Z}^2$ , and  $\inf_{k>0, \boldsymbol{\omega} \in K} |m_0(\mathbf{D}_2^{-k} \boldsymbol{\omega})| > 0$ ,  $\inf_{k>0, \boldsymbol{\omega} \in K} |\widetilde{m_0}(\mathbf{D}_2^{-k} \boldsymbol{\omega})| > 0$ . Further, if  $\sum_{\boldsymbol{\pi} \in \Gamma_0} m_0(\boldsymbol{\omega} + \boldsymbol{\pi}) \widetilde{m_0}(\boldsymbol{\omega} + \boldsymbol{\pi}) = 1$ , then the inverse is true.*

By Theorem 5, the linear system (14) of a bi-orthogonal basis need to satisfy the following identity constraint on  $m_0$  and  $\widetilde{m_0}$ ,

$$m_0 \widetilde{m_0}(\boldsymbol{\omega}) + m_0 \widetilde{m_0}(\boldsymbol{\omega} + \boldsymbol{\pi}_2) + m_0 \widetilde{m_0}(\boldsymbol{\omega} + \boldsymbol{\pi}_4) + m_0 \widetilde{m_0}(\boldsymbol{\omega} + \boldsymbol{\pi}_6) = 1. \quad (15)$$

We thus consider feasible solutions of (14) with constraint (15) using the same approach in [10], which solves compactly supported symmetric bi-orthogonal filters on hexagon lattice. We next review the main scheme in [10] and extend it to our setup of directional wavelet filter.

### 6.1 Summary of Cohen et al's construction

We summarize the main setup and the approach in [10]. Consider a bi-orthogonal scheme consists of 3 high-pass filters  $m_1, m_2$  and  $m_3$  and a low-pass filter  $m_0$

together with their bi-orthogonal duals, s.t.  $m_0$  is  $\frac{2\pi}{3}$ -rotation invariant and  $m_1, m_2, m_3$  are  $\frac{2\pi}{3}$ -rotation co-variant.

This bi-orthogonal scheme satisfies the following linear system ( Lemma 2.2.2 in [10] )

$$\begin{bmatrix} \overline{\widetilde{m}_0(\boldsymbol{\omega})} & \overline{\widetilde{m}_1(\boldsymbol{\omega})} & \overline{\widetilde{m}_2(\boldsymbol{\omega})} & \overline{\widetilde{m}_3(\boldsymbol{\omega})} \\ \overline{\widetilde{m}_0(\boldsymbol{\omega} + \boldsymbol{\nu}_1)} & \overline{\widetilde{m}_1(\boldsymbol{\omega} + \boldsymbol{\nu}_1)} & \overline{\widetilde{m}_2(\boldsymbol{\omega} + \boldsymbol{\nu}_1)} & \overline{\widetilde{m}_3(\boldsymbol{\omega} + \boldsymbol{\nu}_1)} \\ \vdots & \vdots & \vdots & \vdots \\ \overline{\widetilde{m}_0(\boldsymbol{\omega} + \boldsymbol{\nu}_3)} & \overline{\widetilde{m}_1(\boldsymbol{\omega} + \boldsymbol{\nu}_3)} & \overline{\widetilde{m}_2(\boldsymbol{\omega} + \boldsymbol{\nu}_3)} & \overline{\widetilde{m}_3(\boldsymbol{\omega} + \boldsymbol{\nu}_3)} \end{bmatrix} \begin{bmatrix} m_0(\boldsymbol{\omega}) \\ m_1(\boldsymbol{\omega}) \\ m_2(\boldsymbol{\omega}) \\ m_3(\boldsymbol{\omega}) \end{bmatrix} = \begin{bmatrix} 1 \\ 0 \\ 0 \\ 0 \end{bmatrix} \quad (16)$$

or equivalently  $\widetilde{\mathbf{M}} \mathbf{m} = [1, 0, 0, 0]^\top$ , where  $\widetilde{\mathbf{M}} \in \mathbb{C}^{4 \times 4}$  and  $\boldsymbol{\nu}_1 = (\pi, 0), \boldsymbol{\nu}_2 = (0, \pi), \boldsymbol{\nu}_3 = (\pi, \pi)$ .

Given  $\widetilde{m}_1(\boldsymbol{\omega})$ , which by symmetry defines  $\widetilde{m}_2(\boldsymbol{\omega}), \widetilde{m}_3(\boldsymbol{\omega})$ , we can compute  $m_0$ ,

$$\begin{aligned} m_0(\boldsymbol{\omega}) &= D^{-1} \begin{vmatrix} \overline{\widetilde{m}_1(\boldsymbol{\omega} + \boldsymbol{\nu}_1)} & \overline{\widetilde{m}_2(\boldsymbol{\omega} + \boldsymbol{\nu}_1)} & \overline{\widetilde{m}_3(\boldsymbol{\omega} + \boldsymbol{\nu}_1)} \\ \overline{\widetilde{m}_1(\boldsymbol{\omega} + \boldsymbol{\nu}_2)} & \overline{\widetilde{m}_2(\boldsymbol{\omega} + \boldsymbol{\nu}_2)} & \overline{\widetilde{m}_3(\boldsymbol{\omega} + \boldsymbol{\nu}_2)} \\ \overline{\widetilde{m}_1(\boldsymbol{\omega} + \boldsymbol{\nu}_3)} & \overline{\widetilde{m}_2(\boldsymbol{\omega} + \boldsymbol{\nu}_3)} & \overline{\widetilde{m}_3(\boldsymbol{\omega} + \boldsymbol{\nu}_3)} \end{vmatrix} \\ &= D^{-1} \det(\widetilde{\mathbf{M}}_{1,1}(\boldsymbol{\omega})), \quad D \in \mathbb{R}^+ \end{aligned} \quad (17)$$

if  $\widetilde{\mathbf{M}}$  is invertible; both  $m_0(\boldsymbol{\omega})$  and  $\det(\widetilde{\mathbf{M}}_{1,1}(\boldsymbol{\omega}))$ , the minor of  $\widetilde{\mathbf{M}}$  associated with  $\overline{\widetilde{m}_0(\boldsymbol{\omega})}$ , have invariance by  $\frac{2\pi}{3}$ .

*Remark.* For (17) to hold,  $m_0(\boldsymbol{\omega})$  and  $\det(\widetilde{\mathbf{M}}_{1,1}(\boldsymbol{\omega}))$  having the same phase suffices.

If  $\widetilde{m}_0$  is solved, then  $m_1, m_2$  and  $m_3$  are obtained by solving the linear system (16). To get  $\widetilde{m}_0(\boldsymbol{\omega})$ , we solve

$$m_0 \widetilde{m}_0(\boldsymbol{\omega}) + m_0 \widetilde{m}_0(\boldsymbol{\omega} + \boldsymbol{\nu}_1) + m_0 \widetilde{m}_0(\boldsymbol{\omega} + \boldsymbol{\nu}_2) + m_0 \widetilde{m}_0(\boldsymbol{\omega} + \boldsymbol{\nu}_3) = 1 \quad (18)$$

from expanding  $\det(\widetilde{\mathbf{M}})$  with respect to the first column. According to Lemma 3.2.1 in [10] based on *Hilbert's Nullstellensatz*, (18) has a solution iff there does not exist  $(z_1, z_2) \in (\mathbb{C}^*)^2$ ,  $\mathbb{C}^* = \mathbb{C} \setminus \{0\}$  s.t.  $(\pm z_1, \pm z_2)$  are four vanishing points of the  $z$ -transform of  $m_0$ .

### 6.1.1 Solving $\widetilde{m}_0(\boldsymbol{\omega})$

In general, there is no efficient algorithm to solve *Hilbert's Nullstellensatz*, and how (15) is solved exactly is not mentioned in [10].

We propose an optimization approach, where (15) is equivalent to a linear constraint and the objective function imposes regularity on  $\widetilde{m}_0$ . On a  $2N \times 2N$  grid  $\mathcal{G}$  of  $S_0 = [-\pi, \pi) \times [-\pi, \pi)$ , s.t.  $\forall \boldsymbol{\omega}_j \in \mathcal{G}$ ,  $\boldsymbol{\omega}_j + \boldsymbol{\nu}_1, \boldsymbol{\omega}_j + \boldsymbol{\nu}_2, \boldsymbol{\omega}_j + \boldsymbol{\nu}_3 \in \mathcal{G}$ , (15) is reformulated as

$$\mathbf{A} \widetilde{\mathbf{m}}_0 = \mathbf{1}_{4N^2}, \quad (19)$$

$$\widetilde{\mathbf{m}}_0 = [\widetilde{m}_0(\boldsymbol{\omega}_i)]_{i=1, \dots, 4N^2} \quad \mathbf{A}_{i,j} = m_0(\boldsymbol{\omega}_j) \sum_{k=0}^3 \delta(\boldsymbol{\omega}_j - \boldsymbol{\omega}_i - \boldsymbol{\nu}_k)$$

Because the set  $\{\boldsymbol{\omega} + \boldsymbol{\nu}_k, k = 0, 1, 2, 3\}$  is invariant under the shift  $\boldsymbol{\nu}_i, i = 1, 2, 3$ , the rows of  $\mathbf{A}$  corresponding to  $\boldsymbol{\omega}$  and  $\boldsymbol{\omega} + \boldsymbol{\nu}_i$  are identical and we only

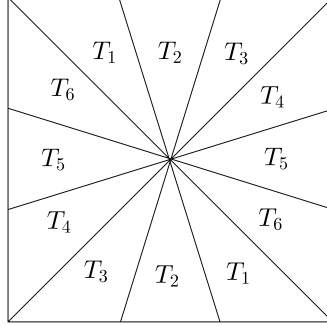


Figure 5: partition of frequency square in six directions, where the essential support of  $\widetilde{m}_i(\boldsymbol{\omega})$  is contained in each pair of triangles  $T_i$

need to consider rows corresponds to  $\boldsymbol{\omega} \in [-\pi, \pi) \times [-\pi, \pi) / \{\boldsymbol{\nu}_i, i = 0, 1, 2, 3\}$ . Therefore,  $\mathbf{A} \in \mathbb{C}^{N^2 \times 4N^2}$  and (19) is under-determinant.

We thus use (19) as a linear constraint in quadratic optimization to solve  $\widetilde{\mathbf{m}}_0$ . Suppose that  $\widetilde{m}_0(\boldsymbol{\omega})$  should be smooth, and we build a differential operator  $\mathbf{D}$  and solve the following minimization problem:

$$\min_{\widetilde{\mathbf{m}}_0} \|\mathbf{D}\widetilde{\mathbf{m}}_0\|^2, \quad s.t. \mathbf{A}\widetilde{\mathbf{m}}_0 = \mathbf{1} \quad (20)$$

or

$$\min_{\widetilde{\mathbf{m}}_0} \|\mathbf{D}\widetilde{\mathbf{m}}_0\|^2 + \lambda \|\mathbf{A}\widetilde{\mathbf{m}}_0 - \mathbf{1}\|^2 \quad (21)$$

The solution of (21) is  $\widetilde{\mathbf{m}}_0 = \lambda(\lambda\mathbf{A}^\top\mathbf{A} + \mathbf{D}^\top\mathbf{D})^{-1}\mathbf{A}^\top\mathbf{1}$ .

Suppose  $\widetilde{m}_0(\boldsymbol{\omega})$  decays away from the origin, then we build a diagonal weighting operator  $\mathbf{W}$ , and solve the following minimization problem:

$$\min_{\widetilde{\mathbf{m}}_0} \|\mathbf{W}\widetilde{\mathbf{m}}_0\|^2, \quad s.t. \mathbf{A}\widetilde{\mathbf{m}}_0 = \mathbf{1} \quad (22)$$

Supplementary numerical results on solving  $\widetilde{m}_0(\boldsymbol{\omega})$  by optimization are provided in Appendix B, where we test this optimization method on pre-designed bi-orthogonal filters  $m_0$  and  $\widetilde{m}_0$ .

## 7 Extension to dilated quincunx scheme

Following the same approach, we focus on the design of  $m_i$ ,  $i = 0, \dots, 6$  and the low pass dual function  $\widetilde{m}_0(\boldsymbol{\omega})$ , given the high pass directional dual functions  $\widetilde{m}_i(\boldsymbol{\omega})$ ,  $i = 1, \dots, 6$ . Assume  $\widetilde{m}_i(\boldsymbol{\omega})$ ,  $i = 1, \dots, 6$  satisfy weak constraints on the direction selectivity of their support.

**Definition.** The *essential support*  $\Omega_i$  of a function  $\widetilde{m}_i$  is the set  $\{\boldsymbol{\omega} : |\widetilde{m}_i(\boldsymbol{\omega})| > |\widetilde{m}_j(\boldsymbol{\omega})|, \forall j \neq i\}$ .

Let pairs of triangles  $T_i$  in Fig.5 contain the essential support of  $\widetilde{m}_i$ ,  $i = 1, \dots, 6$ . A minimum symmetry of  $\widetilde{m}_i(\boldsymbol{\omega})$  is required such that  $\widetilde{m}_1(\boldsymbol{\omega})$  and  $\widetilde{m}_6(\boldsymbol{\omega})$  are symmetric with respect to the diagonal, and so are  $\widetilde{m}_3(\boldsymbol{\omega})$  and  $\widetilde{m}_4(\boldsymbol{\omega})$ .

(14) takes a similar form to (16), but with  $\widetilde{\mathbf{M}} \in \mathbb{C}^{8 \times 7}$ , which is an overdeterminant linear system.

## 7.1 Computing $m_0$

Same as in Section 6.1, we first compute  $m_0$  and assume that  $\widetilde{\mathbf{M}}$  is full rank, otherwise (14) has infinitely many solutions. Moreover,  $\widetilde{\mathbf{M}}[2 : 8, :]$  is singular.

**Lemma 7.1.**  $\widetilde{\mathbf{M}}[2 : 8, :]$  is singular  $\forall \omega$ .

*Proof.* If (14) has a solution, then  $\forall \omega$ ,  $[1, 0, \dots, 0]^\top$  is a linear combination of the columns of  $\widetilde{\mathbf{M}}$  and the solution  $\mathbf{m} \in \text{Null}(\widetilde{\mathbf{M}}[2 : 8, :])$ , hence  $\widetilde{\mathbf{M}}[2 : 8, :]$  being singular is a prerequisite.  $\square$

Therefore, there is a unique row  $\widetilde{\mathbf{M}}[k_\omega, :]$ ,  $k_\omega \in \{2, \dots, 8\}$  such that removing it from  $\widetilde{\mathbf{M}}$  gives a non-singular square matrix  $\widetilde{\mathbf{M}}[-k_\omega, :]$ . By Cramer's rule,

$$m_0(\omega) = \det(\widetilde{\mathbf{M}}_{1,1}[-k_\omega, :]) / \det(\widetilde{\mathbf{M}}[-k_\omega, :]),$$

where  $\det(\widetilde{\mathbf{M}}_{1,1}[-k_\omega, :])$  is the minor of  $\widetilde{\mathbf{M}}[-k_\omega, :]$  associated with  $\widetilde{m}_0(\omega)$ . Let  $C_\omega = \det(\widetilde{\mathbf{M}}[-k_\omega, :])$ , then we have the following observation.

**Lemma 7.2.**  $C_\omega = C_{\omega+\pi_2} = C_{\omega+\pi_4} = C_{\omega+\pi_6}$

*Proof.* Because  $\widetilde{\mathbf{M}}(\omega + \pi_2) = P_{\pi_2} \widetilde{\mathbf{M}}(\omega)$  where  $P_{\pi_2}$  is a row permutation matrix, it follows from the definition of  $C_\omega$  that  $C_\omega = \det(\widetilde{\mathbf{M}}[-k_\omega, :](\omega)) = \det(\widetilde{\mathbf{M}}[-k_{\omega+\pi_2}, :](\omega + \pi_2)) = C_{\omega+\pi_2}$  where  $\mathbf{1}_{k_{\omega+\pi_2}} = P_{\pi_2} \mathbf{1}_{k_\omega}$ .  $\square$

We assume that  $m_0 \in \mathbb{R}_{\geq 0}$  without phase. Let  $m_0^C(\omega) = m_0(\omega)|C_\omega| \in \mathbb{R}_{\geq 0}$  and  $\widetilde{m}_0^C(\omega) = \widetilde{m}_0(\omega)/|C_\omega|$ , then Lemma 7.2 implies the following.

**Proposition 7.3.**  $m_0(\omega)$ ,  $\widetilde{m}_0(\omega)$ ,  $m_i(\omega)$ ,  $i = 1, \dots, 6$  satisfy (14) given  $\widetilde{m}_i(\omega)$ ,  $i = 1, \dots, 6$  if and only if  $m_0^C(\omega)$ ,  $\widetilde{m}_0^C(\omega)$ ,  $m_i(\omega)$ ,  $i = 1, \dots, 6$  do. More generally,  $m_0^C(\omega)c(\omega)$ ,  $\widetilde{m}_0^C(\omega)c(\omega)^{-1}$ ,  $m_i(\omega)$ ,  $i = 1, \dots, 6$  satisfy (14) if  $c(\omega) = c(\omega + \pi_2) = c(\omega + \pi_4) = c(\omega + \pi_6) \neq 0$ .

According to Proposition 7.3, we can first solve  $\widetilde{m}_0^C(\omega)$  and  $m_0^C(\omega)$  and then construct  $c(\omega)$  for optimal  $\widetilde{m}_0(\omega)$  and  $m_0(\omega)$ . In particular,  $m_0^C$  can be computed without knowing  $k_\omega$ ,

$$m_0^C(\omega) = m_0(\omega)|C_\omega| = |\det(\widetilde{\mathbf{M}}_{1,1}[-k_\omega, :])| = \prod_{i=1}^6 \sigma_i(\widetilde{\mathbf{M}}_{1,1}[-k_\omega, :]) = \prod_{i=1}^6 \sigma_i(\widetilde{\mathbf{M}}_{1,1}). \quad (23)$$

In practice, we first perform QR decomposition on  $\widetilde{\mathbf{M}}^\square := \widetilde{\mathbf{M}}_{1,1}$  and then take the absolute value of the product of the diagonal entries of the upper triangular matrix,  $\text{diag}(R)$ . We propose the following algorithm for bi-orthogonal directional filter construction with dilated quincunx downsampling scheme:

**construction of bi-orthogonal basis**

Input:  $\widetilde{m}_i(\omega)$ ,  $i = 1, \dots, 6$

1. compute  $m_0^C(\omega) = \left| \det(\widetilde{\mathbf{M}}_{1,1}[-k_\omega, :]) \right|$
2. compute  $\widetilde{m}_0^C(\omega)$ , such that (14) is solvable and (15) holds
3. solve  $m_i(\omega)$ ,  $i = 1, \dots, 6$  according to (14)
4. design  $c(\omega)$  and let  $m_0(\omega) = m_0^C(\omega)c(\omega)$ ,  $\widetilde{m}_0(\omega) = \widetilde{m}_0^C(\omega)\bar{c}(\omega)^{-1}$

## 7.2 Singularity condition on $\widetilde{\mathbf{M}}[2 : 8, :]$ and discontinuity of $\widetilde{m}_i(\omega)$

Lemma 7.1 is equivalent to the following singularity constraint,

$$0 = \det(\widetilde{\mathbf{M}}[2 : 8, :]) = \widetilde{m}_0(\omega + \pi_2) \det(\widetilde{\mathbf{M}}^\square[-2, :]) + \widetilde{m}_0(\omega + \pi_4) \det(\widetilde{\mathbf{M}}^\square[-4, :]) \\ + \widetilde{m}_0(\omega + \pi_6) \det(\widetilde{\mathbf{M}}^\square[-6, :]).$$

Let  $\widetilde{\mathbf{m}}^i(\omega) = [\widetilde{m}_1(\omega + \pi_i) \cdots, \widetilde{m}_6(\omega + \pi_i)] \in \mathbb{C}^6$ ,  $i = 0, \dots, 7$ , and define  $d_{i,j}(\omega) = \det([\widetilde{\mathbf{m}}^{k_1}(\omega)^\top, \dots, \widetilde{\mathbf{m}}^{k_6}(\omega)^\top])$ ,  $0 \leq k_1 < \dots < k_l < \dots < k_6 \leq 7, k_l \neq i, j$ , then the above singularity condition on  $\widetilde{\mathbf{M}}[2 : 8, :]$  at  $\omega$  can be rewritten as follows,

$$[0, d_{0,2}(\omega), d_{0,4}(\omega), d_{0,6}(\omega)] [\widetilde{m}_0(\omega), \widetilde{m}_0(\omega + \pi_2), \widetilde{m}_0(\omega + \pi_4), \widetilde{m}_0(\omega + \pi_6)]^\top = 0$$

It is easy to verify that the above singular condition at  $\omega + \pi_2$  is equivalent to  $[-d_{0,2}(\omega), 0, d_{2,4}(\omega), d_{2,6}(\omega)] [\widetilde{m}_0(\omega), \widetilde{m}_0(\omega + \pi_2), \widetilde{m}_0(\omega + \pi_4), \widetilde{m}_0(\omega + \pi_6)]^\top = 0$ . Similarly, rewrite the singularity condition at  $\omega + \pi_4$  and  $\omega + \pi_6$  in the coordinate of  $\omega$  and combine all four conditions, we have the following linear constraint

$$\mathfrak{D}(\omega) \begin{bmatrix} \widetilde{m}_0(\omega) \\ \widetilde{m}_0(\omega + \pi_2) \\ \widetilde{m}_0(\omega + \pi_4) \\ \widetilde{m}_0(\omega + \pi_6) \end{bmatrix} = \begin{bmatrix} 0 & d_{0,2} & d_{0,4} & d_{0,6} \\ -d_{0,2} & 0 & d_{2,4} & d_{2,6} \\ -d_{0,4} & -d_{2,4} & 0 & d_{4,6} \\ -d_{0,6} & -d_{2,6} & -d_{4,6} & 0 \end{bmatrix} \begin{bmatrix} \widetilde{m}_0(\omega) \\ \widetilde{m}_0(\omega + \pi_2) \\ \widetilde{m}_0(\omega + \pi_4) \\ \widetilde{m}_0(\omega + \pi_6) \end{bmatrix} = \begin{bmatrix} 0 \\ 0 \\ 0 \\ 0 \end{bmatrix}, \quad (24)$$

where  $\mathfrak{D}(\omega)$  is anti-symmetric. Because  $\mathfrak{D}(\omega)$  is independent of  $m_0(\omega)$ , (24) holds for  $\widetilde{m}_0^C(\omega)$  as well.

On the other hand, given  $m_0(m_0^C)$ ,  $\widetilde{m}_0(\widetilde{m}_0^C)$  has to satisfy the identity constraint (15). (15) and (24) together imply the following proposition,

**Proposition 7.4.** *Given  $\widetilde{m}_i, i = 1, \dots, 6$ , (14) has no solution for any  $\widetilde{m}_0$ , if  $\exists \omega$ , s.t.  $[m_0(\omega), m_0(\omega + \pi_2), m_0(\omega + \pi_4), m_0(\omega + \pi_6)]$  is a linear combination of the rows of  $\mathfrak{D}(\omega)$ .*

Proposition 7.4 provides a necessary condition such that the numerical optimization solving  $\widetilde{m}_0$  is feasible.

**Definition** Let the cone  $T_i = T_i^- \cup T_i^+$ , where  $T_i^-, T_i^+$  are halves of  $T_i$  adjacent to  $T_{i-1}$  and  $T_{i+1}$  respectively.  $\widetilde{m}_i$  concentrates within cone  $T_i$  if  $\text{supp}(\widetilde{m}_i) \subset T_{i-1}^+ \cup T_i \cup T_{i+1}^-$  and  $\int_\Omega |\widetilde{m}_i| > \int_{\Omega'} |\widetilde{m}_i|, \forall \Omega' \subset T_i \cap \text{supp}(\widetilde{m}_i), |\Omega| > 0$ , where  $\Omega'$



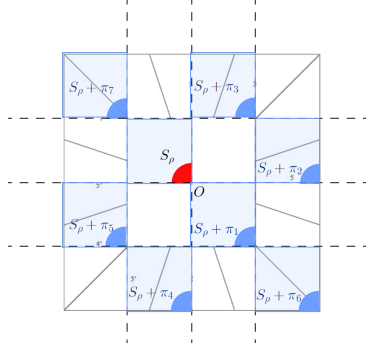


Figure 6:  $S_\rho$  and its shifts

is symmetric to  $\Omega$  with respect to the boundary of  $T_i$ .

Given directional selective  $\widetilde{m}_i(\omega)$  that concentrates in  $T_i$ , we study the feasibility condition in Proposition 7.4 specifically on the domain  $S_\rho = \{(\omega_x, \omega_y) \mid \|\omega\| < \rho, \omega_x < 0, \omega_y < 0\}$ . When  $\rho$  is small enough,  $\widetilde{m}_i(\omega)$  is zero on all but a few sets  $S_\rho + \pi_j$  (see Fig.6 for reference of  $S_\rho$  and its shifts), thus  $\widetilde{\mathbf{m}}^i(\omega)$  is sparse on  $S_\rho$  in the following form

$$\begin{bmatrix} \widetilde{\mathbf{m}}^0 \\ \widetilde{\mathbf{m}}^2 \\ \widetilde{\mathbf{m}}^4 \\ \widetilde{\mathbf{m}}^6 \\ \widetilde{\mathbf{m}}^1 \\ \widetilde{\mathbf{m}}^3 \\ \widetilde{\mathbf{m}}^5 \\ \widetilde{\mathbf{m}}^7 \end{bmatrix} = \begin{bmatrix} 0 & 0 & 0 & 0 & 0 & 0 \\ 0 & * & * & 0 & 0 & 0 \\ 0 & 0 & 0 & * & * & 0 \\ * & 0 & 0 & 0 & 0 & * \\ * & 0 & 0 & 0 & 0 & * \\ 0 & 0 & * & * & 0 & 0 \\ 0 & 0 & * & * & 0 & 0 \\ * & 0 & 0 & 0 & 0 & * \end{bmatrix} = \mathbf{P} \widetilde{\mathbf{M}}[:, 2 : 7], \quad (25)$$

where  $\mathbf{P}$  is a row permutation matrix.

**Lemma 7.5.**  $rank(\widetilde{\mathbf{m}}^1, \widetilde{\mathbf{m}}^7) = 1$  in (25).

*Proof.* We make the following observation of  $\widetilde{\mathbf{m}}^i$  in (25):

- (i)  $\widetilde{\mathbf{m}}^0$  is a zero vector
- (ii)  $\widetilde{\mathbf{m}}^2$  and  $\widetilde{\mathbf{m}}^4$  are linearly independent of each other and the rest of  $\widetilde{\mathbf{m}}^i$
- (iii)  $span\{\widetilde{\mathbf{m}}^1, \widetilde{\mathbf{m}}^6, \widetilde{\mathbf{m}}^7\} \perp span\{\widetilde{\mathbf{m}}^3, \widetilde{\mathbf{m}}^5\}$  and  $rank(\widetilde{\mathbf{m}}^1, \widetilde{\mathbf{m}}^6, \widetilde{\mathbf{m}}^7) \leq 2, rank(\widetilde{\mathbf{m}}^3, \widetilde{\mathbf{m}}^5) \leq 2$

Because  $\widetilde{\mathbf{M}}[2 : 8, 2 : 7]$  consists of rows  $\widetilde{\mathbf{m}}^i, i \neq 0$ , and the low-pass function  $m_0(\omega) \neq 0, \forall \omega \in S_\rho$ , or equivalently  $rank(\widetilde{\mathbf{M}}[2 : 8, 2 : 7](\omega)) = 6$ , it follows from (ii) and (iii) that  $rank(\widetilde{\mathbf{m}}^1, \widetilde{\mathbf{m}}^6, \widetilde{\mathbf{m}}^7) = 2$  and  $rank(\widetilde{\mathbf{m}}^3, \widetilde{\mathbf{m}}^5) = 2$ .

On the other hand, (ii) implies that

$$rank(\widetilde{\mathbf{M}}[2 : 8, 2 : 7](\omega + \pi_2)) = rank(\widetilde{\mathbf{m}}^4, \widetilde{\mathbf{m}}^6, \widetilde{\mathbf{m}}^1, \widetilde{\mathbf{m}}^3, \widetilde{\mathbf{m}}^5, \widetilde{\mathbf{m}}^7) \leq 5$$

and  $\text{rank}(\widetilde{\mathbf{M}}[2 : 8, 2 : 7](\boldsymbol{\omega} + \boldsymbol{\pi}_4)) = \text{rank}(\widetilde{\mathbf{m}}^2, \widetilde{\mathbf{m}}^6, \widetilde{\mathbf{m}}^1, \widetilde{\mathbf{m}}^3, \widetilde{\mathbf{m}}^5, \widetilde{\mathbf{m}}^7) \leq 5$  likewise. Therefore,  $m_0(\boldsymbol{\omega} + \boldsymbol{\pi}_2) = m_0(\boldsymbol{\omega} + \boldsymbol{\pi}_4) = 0$ .

If  $\widetilde{\mathbf{m}}^1$  and  $\widetilde{\mathbf{m}}^7$  are linearly independent, then  $\text{rank}(\widetilde{\mathbf{m}}^2, \widetilde{\mathbf{m}}^4, \widetilde{\mathbf{m}}^1, \widetilde{\mathbf{m}}^3, \widetilde{\mathbf{m}}^5, \widetilde{\mathbf{m}}^7) = 6$  and  $m_0^C(\boldsymbol{\omega} + \boldsymbol{\pi}_6) \neq 0$ , hence  $m_0(\boldsymbol{\omega} + \boldsymbol{\pi}_6) \neq 0$ . Therefore,  $[m_0(\boldsymbol{\omega}), m_0(\boldsymbol{\omega} + \boldsymbol{\pi}_2), m_0(\boldsymbol{\omega} + \boldsymbol{\pi}_4), m_0(\boldsymbol{\omega} + \boldsymbol{\pi}_6)] = [m_0(\boldsymbol{\omega}), 0, 0, m_0(\boldsymbol{\omega} + \boldsymbol{\pi}_6)]$ . In addition,  $d_{i,j} = 0, \forall (i, j)$  except  $(0, 6)$ , so  $\mathfrak{D}(\boldsymbol{\omega}) = [d_{0,6}, 0, 0, 0]^\top [0, 0, 0, 1] + [0, 0, 0, d_{0,6}]^\top [-1, 0, 0, 0]$ . By Prop.7.4, the linear system (14) has no solution  $\forall \widetilde{\mathbf{m}}_0$  and the lemma is proofed.  $\square$

**Lemma 7.6.** *If  $\widetilde{m}_1(\boldsymbol{\omega})(\widetilde{m}_6(\boldsymbol{\omega}))$  concentrates in  $T_1(T_6)$  and its essential support  $\Omega_1 \subset T_1(\Omega_6 \subset T_6)$ , then  $|\widetilde{m}_6(\boldsymbol{\omega})| > |\widetilde{m}_1(\boldsymbol{\omega})|$  a.e. on  $T_6 \cap \text{supp}(\widetilde{m}_6)$  ( $|\widetilde{m}_1(\boldsymbol{\omega})| > |\widetilde{m}_6(\boldsymbol{\omega})|$  a.e. on  $T_1 \cap \text{supp}(\widetilde{m}_1)$ ).*

*Proof* Let  $B_6 = \{\boldsymbol{\omega} : |\widetilde{m}_6(\boldsymbol{\omega})| \leq |\widetilde{m}_1(\boldsymbol{\omega})|, \widetilde{m}_1(\boldsymbol{\omega}) \neq 0\} \cap T_6$  and  $B_1$  be its mirror set with respect to  $\omega_y = \omega_x$  and suppose  $|B_6| > 0$ , then  $\int_{B_6} |\widetilde{m}_6(\boldsymbol{\omega})| \leq \int_{B_6} |\widetilde{m}_1(\boldsymbol{\omega})|$ . Since  $\widetilde{m}_1(\boldsymbol{\omega})$  concentrates in  $T_1$ , we know  $\int_{B_1} |\widetilde{m}_1(\boldsymbol{\omega})| > \int_{B_6} |\widetilde{m}_1(\boldsymbol{\omega})|$ . On the other hand, due to the symmetry of  $\widetilde{m}_1(\boldsymbol{\omega}), \widetilde{m}_6(\boldsymbol{\omega})$  and  $B_1, B_6$ ,  $\int_{B_1} |\widetilde{m}_1(\boldsymbol{\omega})| = \int_{B_6} |\widetilde{m}_6(\boldsymbol{\omega})|$ , hence  $\int_{B_6} |\widetilde{m}_1(\boldsymbol{\omega})| \geq \int_{B_1} |\widetilde{m}_1(\boldsymbol{\omega})|$  which results in contradiction.  $\square$

**Proposition 7.7.** *If  $m_1(m_6)$  concentrates within  $T_1(T_6)$  and  $\Omega_1 \subset T_1(\Omega_6 \subset T_6)$ , then  $\widetilde{m}_1(\boldsymbol{\omega}) = \widetilde{m}_6(\boldsymbol{\omega}) = 0$ , a.e.  $\boldsymbol{\omega} \in S_\rho + \boldsymbol{\pi}_1$ .*

*Proof.* By Lemma 7.6,  $|\widetilde{m}_1(\boldsymbol{\omega})| > |\widetilde{m}_6(\boldsymbol{\omega})|$  a.e. on  $\Omega'_1 := (S_\rho + \boldsymbol{\pi}_7) \cap T_1 = (S_\rho + \boldsymbol{\pi}_1) \cap T_6 + (\pi, \pi)$ . By Lemma 7.5,  $\exists \alpha_\omega \in \mathbb{C}, \text{s.t. } \widetilde{\mathbf{m}}^1(\boldsymbol{\omega}) = \alpha_\omega \widetilde{\mathbf{m}}^7(\boldsymbol{\omega})$ , hence  $|\widetilde{m}_1(\boldsymbol{\omega})| = |\alpha_\omega| \cdot |\widetilde{m}_1(\boldsymbol{\omega} - (\pi, \pi))| \geq |\alpha_\omega| \cdot |\widetilde{m}_6(\boldsymbol{\omega} - (\pi, \pi))| = |\widetilde{m}_6(\boldsymbol{\omega})|$ , a.e. on  $\Omega'_6 := (S_\rho + \boldsymbol{\pi}_1) \cap T_6$ . Therefore,  $\int_{\Omega'_6} |\widetilde{m}_1| \geq \int_{\Omega'_6} |\widetilde{m}_6|$ , which will contradict Lemma 7.6 unless  $|\Omega'_6 \cap \text{supp}(\widetilde{m}_6)| = 0$ , or equivalently  $\alpha_\omega = 0$  and so  $\widetilde{m}_6(\boldsymbol{\omega}) = \widetilde{m}_1(\boldsymbol{\omega}) = 0$ , a.e. on  $(S_\rho + \boldsymbol{\pi}_1) \cap T_6$ . By symmetry,  $\widetilde{m}_6(\boldsymbol{\omega}) = \widetilde{m}_1(\boldsymbol{\omega}) = 0$ , a.e. on  $(S_\rho + \boldsymbol{\pi}_1) \cap T_1$  as well.  $\square$

**Proposition 7.8.**  *$\widetilde{m}_1(\boldsymbol{\omega}), \widetilde{m}_3(\boldsymbol{\omega})$  are not continuous at  $\boldsymbol{\pi}_1, \boldsymbol{\pi}_7$  and  $\widetilde{m}_5(\boldsymbol{\omega}), \widetilde{m}_7(\boldsymbol{\omega})$  are not continuous at  $\boldsymbol{\pi}_3, \boldsymbol{\pi}_5$ .*

*Proof* If  $\widetilde{m}_1(\boldsymbol{\omega})$  is continuous at  $\boldsymbol{\pi}_1$ , then  $\widetilde{m}_1(\boldsymbol{\pi}_1) = \lim_{\alpha \rightarrow 1^-} \widetilde{m}_1(\boldsymbol{\omega}(\alpha)) = 0$ , where  $\{\boldsymbol{\omega}(\alpha), 0 \leq \alpha < 1\} \subset S_\rho + \boldsymbol{\pi}_1$  and  $\boldsymbol{\omega}(1^-) = \boldsymbol{\pi}_1$ . Similarly, we have  $\widetilde{m}_6(\boldsymbol{\pi}_1) = 0$ . Applying the same argument of  $S_\rho$  to its rotation of 180 degree, we have  $\widetilde{m}_1(\boldsymbol{\pi}_7) = \widetilde{m}_6(\boldsymbol{\pi}_7) = 0$ . Therefore  $\widetilde{\mathbf{m}}^1(0) = \widetilde{\mathbf{m}}^7(0) = \mathbf{0}$  and from (23)  $m_0^C(0) = 0$  so that  $m_0(0) = 0$ , which results in contradiction.  $\square$

The following theorem summarizes the necessary condition derived from the singularity condition of  $\widetilde{\mathbf{M}}[2 : 8, :](24)$ .

**Theorem 7.9.** *If  $\widetilde{m}_i(\boldsymbol{\omega})$  concentrates in  $T_i$  with essential support  $\Omega_i \subset T_i$  and  $m_1, m_6$  are symmetric to each other or  $m_3, m_4$  are symmetric to each other, then (14) doesn't have feasible solution given continuous  $\widetilde{m}_i(\boldsymbol{\omega})$ .*

### 7.3 Design of input $\widetilde{m}_i(\omega)$

Following the previous orthonormal construction in Section 4, we consider  $\widetilde{m}_1(\omega), \dots, \widetilde{m}_6(\omega)$  in the form

$$\widetilde{m}_k(\omega) = e^{-i\eta_k^\top \omega} |\widetilde{m}_k(\omega)|, \quad (26)$$

and  $|\widetilde{m}_k(\omega)|$  have certain symmetry. We want to design the phase  $\eta_k$  such that  $m_0(\omega) > 0, \forall \omega \in S_1$ . This is the same as requiring  $\widetilde{\mathbf{M}}^\square$  to be full rank. We first show the necessary conditions on phases  $\eta$  of the full rank requirement on  $\widetilde{\mathbf{M}}^\square$ .

**Lemma 7.10.** *If  $\exists \omega \in D_1 := \{\omega_x = \omega_y, \omega_x \in (-\frac{\pi}{2}, 0)\}$ , s.t.  $m_0(\omega) > 0$ , then  $(\eta_1 - \eta_6)^\top (\pi_6 - \pi_7) \neq 0 \pmod{2\pi}$ .*

*Proof* If  $m_0(\omega) > 0, \omega \in D_1$  then  $\widetilde{\mathbf{M}}^\square$  is full rank, hence its columns are linearly independent. Due to symmetry,  $|\widetilde{m}_1(\omega)| = |\widetilde{m}_6(\omega)|$  on  $\{\omega_x = \omega_y\}$ . Let  $A = |\widetilde{m}_1(\omega + \pi_1)| = |\widetilde{m}_6(\omega + \pi_1)|$  and  $B = |\widetilde{m}_1(\omega + \pi_6)| = |\widetilde{m}_6(\omega + \pi_6)|$ , then the first and the last columns of  $\widetilde{\mathbf{M}}^\square$  are

$$\widetilde{\mathbf{M}}^\square[:, 1] = \begin{bmatrix} 0 \\ \vdots \\ 0 \\ Ae^{i\eta_1^\top (\omega + \pi_6)} \\ Be^{i\eta_1^\top (\omega + \pi_7)} \end{bmatrix} \quad \text{and} \quad \widetilde{\mathbf{M}}^\square[:, 6] = \begin{bmatrix} 0 \\ \vdots \\ 0 \\ Ae^{i\eta_6^\top (\omega + \pi_6)} \\ Be^{i\eta_6^\top (\omega + \pi_7)} \end{bmatrix}.$$

Therefore,  $\widetilde{\mathbf{M}}^\square[:, 1]$  and  $\widetilde{\mathbf{M}}^\square[:, 6]$  are linearly independent implies that  $e^{i(\eta_1 - \eta_6)^\top (\omega + \pi_6)} \neq e^{i(\eta_1 - \eta_6)^\top (\omega + \pi_7)}$  or equivalently  $(\eta_1 - \eta_6)^\top (\pi_6 - \pi_7) \neq 0 \pmod{2\pi}$ .  $\square$

Similarly, if  $\exists \omega \in \{\omega_y = \omega_x, \omega_x \in (0, \frac{\pi}{2})\}$ , s.t.  $m_0(\omega) > 0$ , then  $(\eta_1 - \eta_6)^\top (\pi_6 - \pi_1) \neq 0 \pmod{2\pi}$ . These two conditions are equivalent to

$$(\eta_1 - \eta_6)^\top (\pi/2, \pi/2) \neq 0 \pmod{2\pi} \quad (\text{c1.1})$$

given that  $\eta_1$  and  $\eta_6$  are integer phases. A stronger condition is to require  $\widetilde{\mathbf{M}}^\square[:, 1]$  and  $\widetilde{\mathbf{M}}^\square[:, 6]$  be orthogonal, which is equivalent to

$$(\eta_1 - \eta_6)^\top (\pi/2, \pi/2) = \pi \pmod{2\pi}. \quad (\text{c2.1})$$

Considering the other diagonal segment  $\{\omega_y = -\omega_x, |\omega_x| < \frac{\pi}{2}\}$ , we have

$$(\eta_3 - \eta_4)^\top (-\pi/2, \pi/2) \neq 0 \pmod{2\pi} \quad (\text{c1.2})$$

from the full rank condition and

$$(\eta_3 - \eta_4)^\top (-\pi/2, \pi/2) = \pi \pmod{2\pi} \quad (\text{c2.2})$$

from the stronger orthogonal condition. *Remark* If  $|\widetilde{m}_1(\omega)| = |\widetilde{m}_2(\omega)|$  on  $\{\omega_y = 3\omega_x, |\omega_x| > \frac{\pi}{2}\}$  and  $m_0(\omega) > 0$  on  $\{\omega_y = 3\omega_x \pm \pi, |\omega_y| < \frac{\pi}{2}\}$ , then the same conditions (c1) and (c2) can be derived from full rank and orthogonal conditions respectively for tuples  $(\eta_1, \eta_2, (-\pi/2, \pi/2))$ ,  $(\eta_2, \eta_3, (\pi/2, \pi/2))$ ,  $(\eta_4, \eta_5, (\pi/2, \pi/2))$  and  $(\eta_5, \eta_6, (-\pi/2, \pi/2))$ .

Next, we investigate  $\widetilde{\mathbf{M}}^\square$  at the origin, where the two diagonals meet.

**Proposition 7.11.** *If  $m_0(0) > 0$ , then  $\pi_1^\top (\eta_1 - \eta_6) \neq \pi \pmod{2\pi}$  or  $\pi_3^\top (\eta_3 - \eta_4) \neq \pi \pmod{2\pi}$ .*

*Proof*  $\widetilde{\mathbf{M}}^\square(0)$  takes the following form

$$\begin{bmatrix} * & 0 & 0 & 0 & 0 & * \\ 0 & * & 0 & 0 & 0 & 0 \\ 0 & 0 & * & * & 0 & 0 \\ 0 & 0 & 0 & 0 & * & 0 \\ 0 & 0 & * & * & 0 & 0 \\ * & 0 & * & * & 0 & * \\ * & 0 & 0 & 0 & 0 & * \end{bmatrix}$$

The second and the fifth columns of  $\widetilde{\mathbf{M}}^\square$  have single non-zero entry,  $\widetilde{m}_2(\boldsymbol{\pi}_2)$  and  $\widetilde{m}_5(\boldsymbol{\pi}_4)$  respectively, and are orthogonal to all the rest columns, hence the full-rank constraint of  $\widetilde{\mathbf{M}}^\square$  is reduced to the full-rank constraint on its sub-matrix (with permutation of rows and columns)

$$\overline{\mathbf{B}} := \widetilde{\mathbf{M}}^\square[-2, -4, :] = \begin{bmatrix} \widetilde{m}_1(\boldsymbol{\pi}_6) & \widetilde{m}_6(\boldsymbol{\pi}_6) & \widetilde{m}_3(\boldsymbol{\pi}_6) & \widetilde{m}_4(\boldsymbol{\pi}_6) \\ \widetilde{m}_1(\boldsymbol{\pi}_1) & \widetilde{m}_6(\boldsymbol{\pi}_1) & 0 & 0 \\ \widetilde{m}_1(\boldsymbol{\pi}_7) & \widetilde{m}_6(\boldsymbol{\pi}_7) & 0 & 0 \\ 0 & 0 & \widetilde{m}_3(\boldsymbol{\pi}_3) & \widetilde{m}_4(\boldsymbol{\pi}_3) \\ 0 & 0 & \widetilde{m}_3(\boldsymbol{\pi}_5) & \widetilde{m}_4(\boldsymbol{\pi}_5) \end{bmatrix}$$

Without loss of generality, let  $|\widetilde{m}_1(\boldsymbol{\pi}_1)| = |\widetilde{m}_1(\boldsymbol{\pi}_7)| = |\widetilde{m}_6(\boldsymbol{\pi}_1)| = |\widetilde{m}_6(\boldsymbol{\pi}_7)| = |\widetilde{m}_3(\boldsymbol{\pi}_3)| = |\widetilde{m}_3(\boldsymbol{\pi}_5)| = |\widetilde{m}_4(\boldsymbol{\pi}_3)| = |\widetilde{m}_4(\boldsymbol{\pi}_5)| = a$  and  $|\widetilde{m}_1(\boldsymbol{\pi}_6)| = |\widetilde{m}_6(\boldsymbol{\pi}_6)| = |\widetilde{m}_3(\boldsymbol{\pi}_6)| = |\widetilde{m}_4(\boldsymbol{\pi}_6)| = b$ . Rewrite  $\overline{\mathbf{B}}$  as follows,

$$\overline{\mathbf{B}} = \begin{bmatrix} be^{-i\boldsymbol{\pi}_6^\top \boldsymbol{\eta}_1} & be^{-i\boldsymbol{\pi}_6^\top \boldsymbol{\eta}_6} & be^{-i\boldsymbol{\pi}_6^\top \boldsymbol{\eta}_3} & be^{-i\boldsymbol{\pi}_6^\top \boldsymbol{\eta}_4} \\ ae^{-i\boldsymbol{\pi}_1^\top \boldsymbol{\eta}_1} & ae^{-i\boldsymbol{\pi}_1^\top \boldsymbol{\eta}_6} & 0 & 0 \\ ae^{i\boldsymbol{\pi}_1^\top \boldsymbol{\eta}_1} & ae^{i\boldsymbol{\pi}_1^\top \boldsymbol{\eta}_6} & 0 & 0 \\ 0 & 0 & ae^{-i\boldsymbol{\pi}_3^\top \boldsymbol{\eta}_3} & ae^{-i\boldsymbol{\pi}_3^\top \boldsymbol{\eta}_4} \\ 0 & 0 & ae^{i\boldsymbol{\pi}_3^\top \boldsymbol{\eta}_3} & ae^{i\boldsymbol{\pi}_3^\top \boldsymbol{\eta}_4} \end{bmatrix}$$

The product of singular values of  $\mathbf{B}$  is

$$\sqrt{\det(\mathbf{B}^* \mathbf{B})} = 4a^3 \sqrt{a^2 K_1^2 K_2^2 + b^2 (Q_1 K_2^2 + Q_2 K_1^2)}, \quad (27)$$

where  $Q_1 = 1 - \cos(\boldsymbol{\pi}_6^\top (\boldsymbol{\eta}_1 - \boldsymbol{\eta}_6)) \cos(\boldsymbol{\pi}_1^\top (\boldsymbol{\eta}_1 - \boldsymbol{\eta}_6))$ ,  $Q_2 = 1 - \cos(\boldsymbol{\pi}_6^\top (\boldsymbol{\eta}_3 - \boldsymbol{\eta}_4)) \cos(\boldsymbol{\pi}_3^\top (\boldsymbol{\eta}_3 - \boldsymbol{\eta}_4))$ ,  $K_1 = \sin(\boldsymbol{\pi}_1^\top (\boldsymbol{\eta}_1 - \boldsymbol{\eta}_6))$ ,  $K_2 = \sin(\boldsymbol{\pi}_3^\top (\boldsymbol{\eta}_3 - \boldsymbol{\eta}_4))$ .

If the previous strong orthogonal condition on  $\boldsymbol{\eta}_1, \boldsymbol{\eta}_3, \boldsymbol{\eta}_4, \boldsymbol{\eta}_6$  holds, then  $K_1 = K_2 = 0$  and  $m_0(0) = m_0^C(0) = 0$ . Therefore, the strong orthogonal condition (c2) cannot be satisfied at the same time. In particular, we consider the following constraints on phase  $\boldsymbol{\eta}_k \in \mathbb{Z}^2$ ,  $k = 1, \dots, 6$ :

$$\begin{aligned} (\boldsymbol{\eta}_1 - \boldsymbol{\eta}_2)^\top (-\pi/2, \pi/2) &= (\boldsymbol{\eta}_5 - \boldsymbol{\eta}_6)^\top (-\pi/2, \pi/2) = \pi \pmod{2\pi} \\ (\boldsymbol{\eta}_2 - \boldsymbol{\eta}_3)^\top (\pi/2, \pi/2) &= (\boldsymbol{\eta}_4 - \boldsymbol{\eta}_5)^\top (\pi/2, \pi/2) = \pi \pmod{2\pi} \\ (\boldsymbol{\eta}_3 - \boldsymbol{\eta}_4)^\top (-\pi/2, \pi/2) &= -\pi/2 \pmod{2\pi} \quad (\boldsymbol{\eta}_6 - \boldsymbol{\eta}_1)^\top (\pi/2, \pi/2) = \pi/2 \pmod{2\pi} \end{aligned} \quad (28)$$

where we require strong orthogonal constraints on pair of shifts corresponding to  $\widetilde{m}$  function with non-diagonal common boundary and weaker constraints on

$(\boldsymbol{\eta}_1, \boldsymbol{\eta}_6)$  and  $(\boldsymbol{\eta}_3, \boldsymbol{\eta}_4)$ . A solution to (28) is

$$\begin{aligned}\boldsymbol{\eta}_1 &= (0, 0), \quad \boldsymbol{\eta}_2 = (-1, 1), \quad \boldsymbol{\eta}_3 = (0, 2), \\ \boldsymbol{\eta}_4 &= (1, 0), \quad \boldsymbol{\eta}_5 = (0, -1), \quad \boldsymbol{\eta}_6 = (0, 1).\end{aligned}\tag{29}$$

#### 7.4 solving $m_i$

In the final step, we substitute  $\widetilde{m}_0^C(\boldsymbol{\omega})$  and  $m_0^C(\boldsymbol{\omega})$  into (14) and rewrite it into the following linear system,

$$\widetilde{\mathbf{M}}[:, 2 : 7] \mathbf{m}[2 : 7](\boldsymbol{\omega}) = \begin{bmatrix} 1 - m_0^C \overline{\widetilde{m}_0^C}(\boldsymbol{\omega}) \\ 0 \\ -m_0^C \overline{\widetilde{m}_0^C}(\boldsymbol{\omega} + \boldsymbol{\pi}_2) \\ \vdots \\ 0 \end{bmatrix} =: \mathbf{b}(\boldsymbol{\omega}). \tag{30}$$

The solution of (30) depends only on  $m_0^C \overline{\widetilde{m}_0^C}$ , or equivalently  $m_0 \overline{\widetilde{m}_0}$ .

## 8 Numerical Experiments

### 8.1 solving $m_0^C$

A set of  $\widetilde{m}_i(\boldsymbol{\omega})$  that satisfy the conditions of Theorem 7.9 with phase terms in (29) is used as the input of (14). The left figure in Fig.7 shows the absolute value of  $\widetilde{m}_i(\boldsymbol{\omega})$ . In particular,  $\widetilde{m}_i(\boldsymbol{\omega}) = 0, \forall \boldsymbol{\omega} \in S_1$ . We follow the construction process in Section 7.1 and obtain  $m_0^C$  shown in the right of Fig.7, in both normal scale and log scale. We perform a numerical sanity check on the necessary condition in Proposition 7.4, that is  $\forall \boldsymbol{\omega}, s.t. [m_0(\boldsymbol{\omega}), m_0(\boldsymbol{\omega} + \boldsymbol{\pi}_2), m_0(\boldsymbol{\omega} + \boldsymbol{\pi}_4), m_0(\boldsymbol{\omega} + \boldsymbol{\pi}_6)]$  is not a linear combination of the rows of  $\mathfrak{D}(\boldsymbol{\omega})$  in (24). Equivalently, we compute the following quantity

$$\vartheta = 1 - \|V^\top \mathbf{m}_0\| / \|\mathbf{m}_0\|,$$

where  $\mathbf{m}_0(\boldsymbol{\omega}) = [m_0(\boldsymbol{\omega}), m_0(\boldsymbol{\omega} + \boldsymbol{\pi}_2), m_0(\boldsymbol{\omega} + \boldsymbol{\pi}_4), m_0(\boldsymbol{\omega} + \boldsymbol{\pi}_6)]^\top$  and  $V$  are the left singular vectors of  $\mathfrak{D}(\boldsymbol{\omega})$  whose corresponding singular values are non-zero. If  $\mathbf{m}_0 \in \text{span}(V)$ , then  $\vartheta = 0$ . If  $\mathbf{m}_0 \perp \text{span}(V)$ , then  $\vartheta = 1$ . Fig.8 shows the feasibility check  $\vartheta$  of input  $\widetilde{m}_i(\boldsymbol{\omega})$ , and  $\mathbf{m}_0$  is orthogonal to  $\text{span}(V)$  everywhere.

### 8.2 solving $\widetilde{m}_0^C(\boldsymbol{\omega})$ and $m_i$

We compute  $\widetilde{m}_0^C(\boldsymbol{\omega})$  by solving the following optimization problem similar to (20) for the dyadic scheme,

$$\min_{\mathbf{x}} \|\mathbf{D}(\mathbf{m}_0^C \circ \mathbf{x})\|^2 + \lambda \|\mathbf{w} \circ \mathbf{m}_0^C \circ \mathbf{x}\|^2, \quad s.t. \mathbf{A}\mathbf{x} = \mathbf{1}, \mathfrak{D}\mathbf{x} = \mathbf{0} \tag{31}$$

where  $\circ$  is Hadamard product and  $\mathbf{w}$  is a weight vector and we consider real solution  $\mathbf{x}$  here.  $\mathbf{A}$  in the constraint is the matrix generated from the identity condition (15) and  $\mathfrak{D}$  is generated from the singularity condition (24). Since  $\mathbf{A}$  and  $\mathfrak{D}$  are linearly independent, (31) is feasible. Here, instead of optimizing the

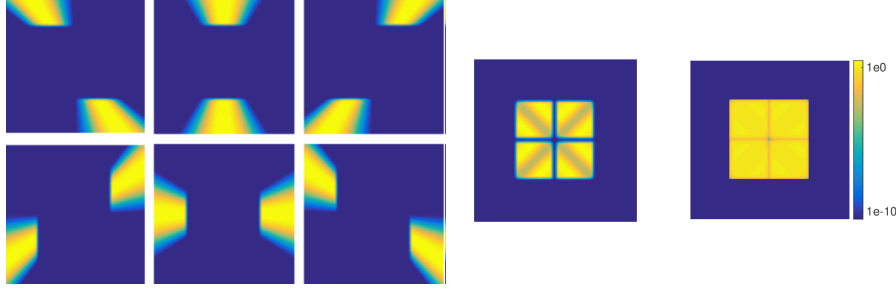


Figure 7: Left:  $|\widetilde{m}_i(\omega)|$ , middle: computed  $m_0^C$ , right:  $\log(m_0^C)$

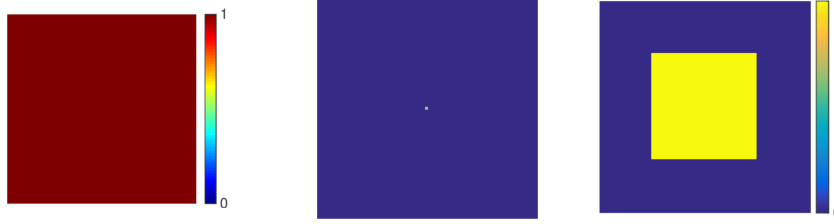


Figure 8:  $\vartheta$

Figure 9: Left: : computed  $\widetilde{m}_0^C$ , right:  $\widetilde{m}_0^C \cdot m_0^C$

properties of  $\mathbf{x}$  as in (20), we optimize those of  $\widetilde{\mathbf{m}}_0^C \circ \mathbf{x}$  since  $m_0^C \cdot \widetilde{m}_0^C$  will be later re-decomposed into  $m_0$  and  $\widetilde{m}_0$ . In addition, if  $m_0^C$  is symmetric with respect to the two coordinates  $\omega_x$  and  $\omega_y$ , then we impose the same symmetry on  $\widetilde{m}_0^C$  by solving (31) on  $[0, \pi) \times [0, \pi)$  and then extend the solution to  $[-\pi, \pi) \times [-\pi, \pi)$  by symmetry.

Fig.9 shows  $\widetilde{m}_0^C(\omega)$  obtained from (31) and  $\widetilde{m}_0^C \cdot m_0^C$  which is  $\mathbf{1}_{S_1}$ .

In particular, given  $\widetilde{m}_0^C \cdot m_0^C = 1$ ,  $\mathbf{b}(\omega) = \mathbf{0}$ ,  $\forall \omega \in S_1$ , hence  $\mathbf{m}[2 : 7] = \mathbf{0}$ . When  $\mathbf{b}(\omega) \neq \mathbf{0}$ , (30) is a degenerated over-determinant linear system (we also do a sanity check here for the linearity between  $\widetilde{\mathbf{M}}[:, 2 : 7]$  and  $\mathbf{b}$  by computing  $\vartheta$ ) and

$$\mathbf{m}[2 : 7](\omega) = \left( \widetilde{\mathbf{M}}[:, 2 : 7] \right)^\dagger \mathbf{b}(\omega),$$

where  $\dagger$  is the pseudo-inverse of a matrix. Fig.10 shows the solution  $m_i$  of (30) and the corresponding spatial filters  $\mathcal{F}^{-1}\widetilde{m}_0$ . As shown in Fig.10, the energy of  $m_i$  concentrates on  $\{|\omega_x| = \frac{\pi}{2}, |\omega_y| = \frac{\pi}{2}\}$  where  $|\widetilde{m}_i|$  is small, and the filters decay slowly in time domain.

The bi-orthogonal bases constructed is not ideal, despite the regularization on  $m_0$  in the optimization (31). Since no explicit regularization is put on  $m_i$ , it's difficult to control the regularity of the output  $m_i$  from the input  $\widetilde{m}_i$ .

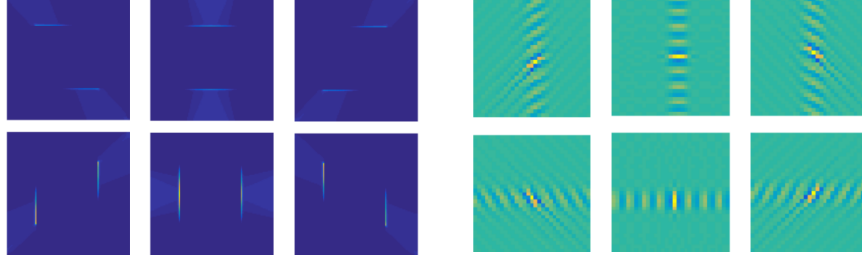


Figure 10: Left:  $|m_i|$ ,  $i = 1, \dots, 6$ , right:  $|\mathcal{F}^{-1}m_i|$

## 9 Conclusion

In this paper, we consider directional wavelet schemes on dilated quincunx sublattice and analyze their regularity. We show that filters in both orthonormal and bi-orthogonal bases have discontinuity in the frequency domain at the corners of  $S_1 = [-\pi/2, \pi/2) \times [-\pi/2, \pi/2)$ , hence they cannot be not well localized in the time domain.

Our analysis is closely related to our proposed bases construction algorithms, and we show that the construction method of orthonormal bases can be easily extended to build frames construction of redundancy 2, which achieve much better time frequency localization and thus practically useful. The bi-orthogonal construction takes a different approach from the orthonormal case, where directional dual filters are first designed such that they can be completed to a bi-orthogonal frame and the remaining filters are obtained by solving feasible linear systems or quadratic optimization. Its extension to low-redundancy dual frame construction is not studied here and will be our future focus.

# Appendices

## A Proof of Theorem 1

Take the Fourier transform of both sides of (5), we have

$$\begin{aligned} \sum_{\mathbf{k}} \langle f, \phi_{\mathbf{k}} \rangle \hat{\phi}(\boldsymbol{\omega}) e^{-i\boldsymbol{\omega}^T \mathbf{k}} &= \sum_{\mathbf{k}} \langle f, \phi_{1,\mathbf{k}} \rangle e^{-i\boldsymbol{\omega}^T \mathbf{D}_2 \mathbf{k}} |\mathbf{D}_2|^{1/2} \hat{\phi}(\mathbf{D}_2^T \boldsymbol{\omega}) \\ &\quad + \sum_{j=1}^J \sum_{\mathbf{k}} \langle f, \psi_{1,\mathbf{k}}^j \rangle e^{-i\boldsymbol{\omega}^T \mathbf{D} \mathbf{k}} |\mathbf{D}|^{1/2} \hat{\phi}(\mathbf{D}^T \boldsymbol{\omega}) \end{aligned}$$

Suppose  $m_j$  are trigonometric series

$$m_0(\boldsymbol{\omega}) = \sum_{\mathbf{k}} c_{\mathbf{k}} e^{-i\boldsymbol{\omega}^T \mathbf{k}} \quad m_j(\boldsymbol{\omega}) = \sum_{\mathbf{k}} g_{\mathbf{k}} e^{-i\boldsymbol{\omega}^T \mathbf{k}}, \quad j = 1, \dots, J \quad (32)$$

The first term on the right hand side can be represented by  $\hat{\phi}(\omega)$  and  $\langle f, \phi_k \rangle$  using (1) and (32).

$$\begin{aligned}
\text{the first term on R.H.S.} &= \sum_{\mathbf{k}} \langle f, \phi_{1,\mathbf{k}} \rangle e^{-i\omega^T \mathbf{D}_2 \mathbf{k}} |\mathbf{D}_2|^{1/2} m_0(\omega) \hat{\phi}(\omega) \\
&= \sum_{\mathbf{k}} \left( \sum_{\mathbf{k}'} \langle f, \phi_{\mathbf{k}'} \rangle \overline{c_{\mathbf{k}' - \mathbf{D}_2 \mathbf{k}}} |\mathbf{D}_2|^{1/2} \right) e^{-i\omega^T \mathbf{D}_2 \mathbf{k}} |\mathbf{D}_2|^{1/2} m_0(\omega) \hat{\phi}(\omega) \\
&= \sum_{\mathbf{k}'} \langle f, \phi_{\mathbf{k}'} \rangle \left( |\mathbf{D}_2| \sum_{\mathbf{k}} \overline{c_{\mathbf{k}' - \mathbf{D}_2 \mathbf{k}}} e^{i\omega^T (\mathbf{k}' - \mathbf{D}_2 \mathbf{k})} \right) e^{-i\omega^T \mathbf{k}'} m_0(\omega) \hat{\phi}(\omega).
\end{aligned}$$

*Remark.* If we have a shift  $\mathbf{k}_0$  in the down-sample scheme, i.e.  $\mathbf{D}_2 \mathbb{Z}^2 - \mathbf{k}_0$  instead of  $\mathbf{D}_2 \mathbb{Z}^2$ , so that we obtain coefficient of  $\hat{\phi}_{1,\mathbf{k}} = \phi_{1,\mathbf{k} + \mathbf{k}_0}$  instead of  $\phi_{1,\mathbf{k}}$ , and  $\hat{\phi}_1(\mathbf{x}) = \phi_1(\mathbf{x} - \mathbf{k}_0) = |\mathbf{D}_2|^{1/2} \sum_{\mathbf{k}} c_{\mathbf{k}} \phi(\mathbf{x} - \mathbf{k} - \mathbf{k}_0) = |\mathbf{D}_2|^{1/2} \sum_{\mathbf{k}} c_{\mathbf{k} - \mathbf{k}_0} \phi(\mathbf{x} - \mathbf{k})$ . This change of down-sample scheme results in an extra phase term  $e^{-i\omega^T \mathbf{k}_0}$  in  $m_0$ . Here, we use the down-sample scheme without translation.

Since  $\bigcup_{\beta \in B} \{\beta\} := \bigcup_{\beta \in B} (\mathbf{D}_2 \mathbb{Z}^2 + \beta) = \mathbb{Z}^2$ , where  $B = \{(0, 0), (1, 0), (0, 1), (1, 1)\}$ , the summation over  $\mathbf{k}' \in \mathbb{Z}^2$  can be written as a double sum  $\sum_{\beta \in B} \sum_{\mathbf{k}' \in \{\beta\}}$ ,

$$\begin{aligned}
&\sum_{\beta \in B} \sum_{\mathbf{k}' \in \{\beta\}} \langle f, \phi_{\mathbf{k}'} \rangle \sum_{\mathbf{k}} \overline{c_{\mathbf{k}' - \mathbf{D}_2 \mathbf{k}}} e^{i\omega^T (\mathbf{k}' - \mathbf{D}_2 \mathbf{k})} e^{-i\omega^T \mathbf{k}'} |\mathbf{D}_2| m_0(\omega) \hat{\phi}(\omega) \\
&= \sum_{\beta \in B} \sum_{\mathbf{k}' \in \{\beta\}} \langle f, \phi_{\mathbf{k}'} \rangle \sum_{\mathbf{k} \in \{\beta\}} \overline{c_{\mathbf{k}}} e^{i\omega^T \mathbf{k}} e^{-i\omega^T \mathbf{k}'} |\mathbf{D}_2| m_0(\omega) \hat{\phi}(\omega)
\end{aligned}$$

The summation over  $\mathbf{k}$  in the middle is similar to the trigonometric form of  $m_0$  in (32), but  $\mathbf{k}$  takes value on the shifted sub-lattice  $\{\beta\}$  instead of  $\mathbb{Z}^2$ . Therefore, the summation equals to instead a linear combination of  $m_0$  with shifts  $\Gamma_0$ ,

$$\sum_{\pi \in \Gamma_0} m_0(\omega + \pi) e^{i\beta^T \pi} = \sum_{\mathbf{k} \in \{\beta\}} c_{\mathbf{k}} e^{-i\omega^T \mathbf{k}} \quad (33)$$

Substitute (33) into the previous expression,

$$\sum_{\beta \in B} \sum_{\mathbf{k}' \in \{\beta\}} \langle f, \phi_{\mathbf{k}'} \rangle \sum_{\pi \in \Gamma_0} \overline{m_0(\omega + \pi)} e^{-i\beta^T \pi} e^{-i\omega^T \mathbf{k}'} m_0(\omega) \hat{\phi}(\omega)$$

Since  $e^{i\pi^T \beta} = e^{i\pi^T \mathbf{k}'}$ ,  $\forall \mathbf{k}' \in \{\beta\}$ , after rewriting the double sum over  $\mathbf{k}'$  back to a unit sum on  $\mathbb{Z}^2$ , we get

$$\sum_{\mathbf{k}'} \langle f, \phi_{\mathbf{k}'} \rangle e^{-i\omega^T \mathbf{k}'} \hat{\phi}(\omega) \left( \sum_{\pi \in \Gamma_0} \overline{m_0(\omega + \pi)} m_0(\omega) e^{-i\pi^T \mathbf{k}'} \right)$$

Similarly, the second term on the R.H.S. of (5) equals to

$$\sum_{j=1}^J \sum_{\mathbf{k}'} \langle f, \phi_{\mathbf{k}'} \rangle e^{-i\omega^T \mathbf{k}'} \hat{\phi}(\omega) \left( \sum_{\pi \in \Gamma_1} \overline{m_j(\omega + \pi)} m_j(\omega) e^{-i\pi^T \mathbf{k}'} \right)$$

(For Theorem 3 on frame construction, the summation of shifts  $\pi$  is over  $\Gamma_0$  instead of  $\Gamma_1$ .) Combining the two terms on the R.H.S. of (5), and compare the coefficients of  $\langle f, \phi_{\mathbf{k}'} \rangle e^{-i\omega^T \mathbf{k}'} \hat{\phi}(\omega)$  on both sides, the perfect reconstruction



condition is then equivalent to  $\forall \mathbf{k}'$ ,

$$\sum_{\boldsymbol{\pi} \in \Gamma_0} e^{-i\boldsymbol{\pi}^T \mathbf{k}'} \overline{m_0(\boldsymbol{\omega} + \boldsymbol{\pi})} m_0(\boldsymbol{\omega}) + \sum_j \sum_{\boldsymbol{\pi} \in \Gamma_1} e^{-i\boldsymbol{\pi}^T \mathbf{k}'} \overline{m_j(\boldsymbol{\omega} + \boldsymbol{\pi})} m_j(\boldsymbol{\omega}) = 1.$$

This is equivalent to

$$|m_0(\boldsymbol{\omega})|^2 + \sum_j |m_j(\boldsymbol{\omega})|^2 = 1$$

and

$$\begin{aligned} \sum_{j=0}^J \overline{m_j(\boldsymbol{\omega} + \boldsymbol{\pi})} m_j(\boldsymbol{\omega}) &= 0, \boldsymbol{\pi} \in \Gamma_0 \setminus \{\mathbf{0}\} \\ \sum_{j=1}^J \overline{m_j(\boldsymbol{\omega} + \boldsymbol{\pi})} m_j(\boldsymbol{\omega}) &= 0, \boldsymbol{\pi} \in \Gamma_1 \setminus \Gamma_0 \end{aligned}$$

*Remark.* Because each  $m_j$  is  $(2\pi, 2\pi)$  periodic, we only need to check the above equality  $\forall \boldsymbol{\omega} \in S_0$ . If we downsample  $\psi_1^j$  on a shifted sub-lattice  $D\mathbb{Z}^2 - \mathbf{k}_j$ , we then have an extra phase  $e^{i\boldsymbol{\pi}^T \mathbf{k}_j}$  before  $\overline{m_j(\boldsymbol{\omega} + \boldsymbol{\pi})} m_j(\boldsymbol{\omega})$  in shift cancellation condition. This provides additional freedom in the construction yet it is not substantial.

## B Supplementary Numerical Results

### B.1 Numerical optimization of $\widetilde{m}_0(\boldsymbol{\omega})$ in 1D

To test whether numerical optimization is a practical way to solve (18), we first experiment on  $m_0(\boldsymbol{\omega})$  and  $\widetilde{m}_0(\boldsymbol{\omega})$  of pre-designed bi-orthogonal wavelets. We consider a low frequency filters corresponding to bi-orthogonal scaling functions  $\phi, \tilde{\phi}$  with vanishing moments 3 and 5 respectively.

The filters are shown in Fig.11. Suppose we know the upper decomposition filter, and we want to find the lower reconstruction filter by solving (18), such that the filter has support as compact as possible. The corresponding  $m_0$  and  $\widetilde{m}_0$  are complex, yet we can shift the phase of  $m_0$  such that  $m_0$  is real and apply the same phase shift to  $\widetilde{m}_0(\boldsymbol{\omega})$ . Without loss of generality, (18) can be solved assuming that  $m_0$  is real. It is not necessary that the corresponding  $\widetilde{m}_0$  is also real, but in this testing case,  $m_0(\boldsymbol{\omega})$  and  $\widetilde{m}_0(\boldsymbol{\omega})$  have the same phase, hence the phase-shifted  $\widetilde{m}_0(\boldsymbol{\omega})$  is real as well. Fig.12 shows the ground truth  $m_0(\boldsymbol{\omega})$  and  $\widetilde{m}_0(\boldsymbol{\omega})$  considered in this simulation.

Let  $\widetilde{\widetilde{m}}_0(\boldsymbol{\omega})$  be the approximation of  $\widetilde{m}_0(\boldsymbol{\omega})$ , which is solution of the following

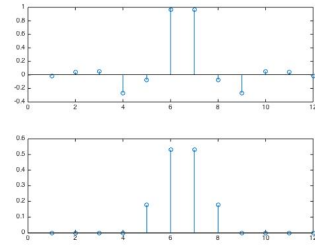


Figure 11: 1d filters, up: LoD, down: LoR

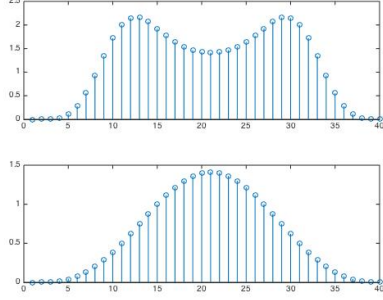


Figure 12:  $m_0(\omega)$  and  $\widetilde{m}_0(\omega)$

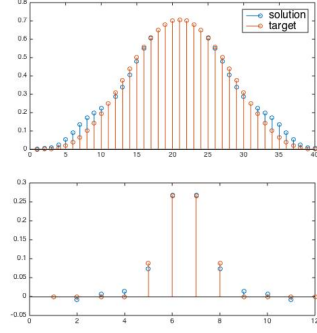


Figure 13:  $\widehat{m}_0(\omega)$  vs.  $\widetilde{m}_0(\omega)$

optimization problem

$$\min_{\mathbf{x}} \|\mathbf{D}\mathbf{x}\|^2 + \|\mathbf{x}\|^2, \quad s.t. \mathbf{A}\mathbf{x} = \mathbf{1} \quad (34)$$

where  $\mathbf{A}$  in the constraint is the matrix generated from (15) (in 1D, only a single shift of  $\pi$  appears in the condition, so each row of  $\mathbf{A}$  has two non-zero entries). Notice that no symmetry constraint is imposed here, nevertheless, the solution shown in Fig.13 is almost symmetric. On the other hand, its support in the time domain is not as compact as that of  $\widetilde{m}_0(\omega)$ , see the bottom of Fig.13.

## B.2 Numerical optimization of $\widetilde{m}_0(\omega)$ in 2D

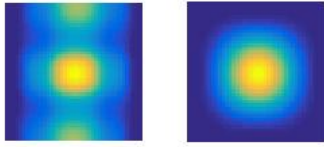


Figure 14: Left: result of (34) in 2D, Right: target

The 2D case is much harder and several different optimization problems are formulated and their solutions are shown in the following. The 2D bi-orthogonal low-pass filters used here are the tensor products of the 1D filters used above. *2D version of (34)*

The 1D formulation can be easily extended to 2D, where  $\mathbf{D} = [\mathbf{D}_x, \mathbf{D}_y]$  consider 1st order derivative in both  $x$  and  $y$  directions, and  $\mathbf{A}$  is generated from (15), each row has four non-zero entries. Fig.14 shows the minimizer and compares it with the target function. It is obvious that the solution is not 90°-rotation invariant. Even worse is the fact that there is much energy in the vertical high-frequency domain.

To enforce the support of  $\widehat{m}_0(\omega)$  concentrates within the low frequency domain, the squared  $\ell_2$ -norm regulator in (34) is changed to a weighted version

(corresponding to Modulation space) as follows,

$$\min_{\mathbf{x}} \|\mathbf{D}\mathbf{x}\|^2 + \lambda \|\mathbf{w} \circ \mathbf{x}\|^2, \quad s.t. \mathbf{A}\mathbf{x} = \mathbf{1} \quad (35)$$

where  $\circ$  is Hadamard product and  $\mathbf{w}$  is a weight vector. In particular, we choose  $\forall \omega, \mathbf{w}(\omega) = \|\omega\|$ . Fig.15 and Fig.16 show the minimizer of (35) with  $\lambda = 60$  and 600 respectively. As  $\lambda$  increases, the support of the minimizer concentrates more within the low frequency region. As shown in Fig.15, when  $\lambda$  is not huge, the minimizer achieves a certain level of but not full symmetry, whereas Fig.16 shows that huge  $\lambda$  imposes full symmetry.

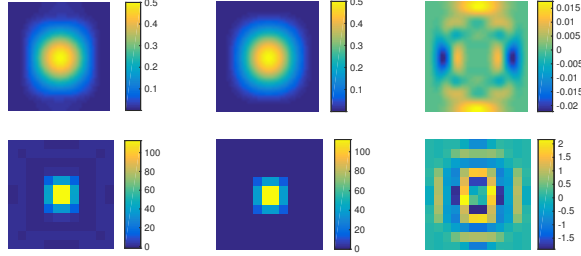


Figure 15: result of (35)  $\widehat{m}_0(\omega)$  ( $\lambda = 60$ ), target  $\widehat{m}_0(\omega)$  and their difference, Top: frequency domain, Bottom: time domain

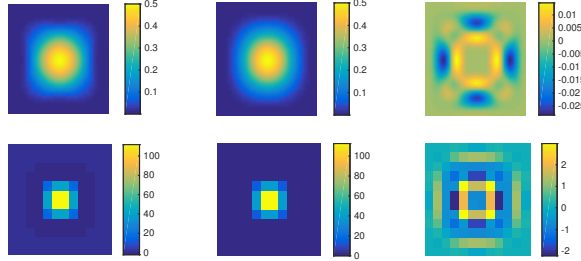


Figure 16: result of (35)  $\widehat{m}_0(\omega)$  ( $\lambda = 600$ ), target  $\widehat{m}_0(\omega)$  and their difference

*weighted L2 norm with symmetry constraint*

If we hard constrain the symmetry by the following

$$\min_{\mathbf{x}} \|\mathbf{D}\mathbf{x}\|^2 + \lambda \|\mathbf{w} \circ \mathbf{x}\|^2, \quad s.t. \mathbf{A}\mathbf{x} = \mathbf{1}, \mathbf{S}\mathbf{x} = \mathbf{0} \quad (36)$$

where each row of  $\mathbf{S}$  has an one entry and a negative one entry at the location of two points have the same value due to symmetry. In practice, we put symmetry constraints such that the upper half plane is symmetric to the lower half plane w.r.t.  $x$  coordinate and the first quadrant is  $90^\circ$ -rotational invariant w.r.t. the second quadrant. The symmetry constraint makes the optimization problem significantly harder, resulting in longer optimization algorithm running time and no near-optimal solution is found (the algorithm terminates as the maxi-

mum number of iterations is exceeded). Fig.17 shows the result provided by the Matlab quadratic minimization solver, unfortunately, there are artifacts at the near endpoints of  $x$  and  $y$  coordinates.

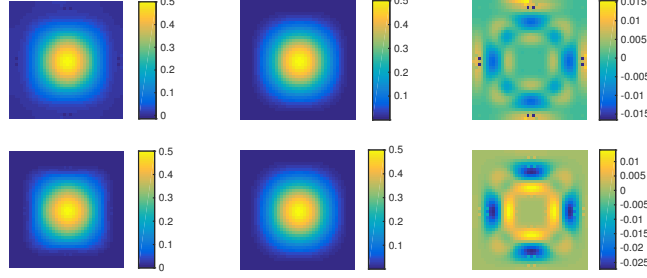


Figure 17: solution of (36) (top:  $\lambda = 60$ , bottom:  $\lambda = 600$ ) provided by Matlab solver `quadprog`

On the other hand, asymmetric solution can always be symmetrized by the average of the solution and its dual w.r.t. rotation, mirroring, etc. This approach increase the support of the solution, thus a well concentrated solution in the frequency domain is necessary to begin with.

#### *Other potential formulations*

We may also putting weights in the first L2-norm of derivatives, such that

$$\min_{\mathbf{x}} \|\mathbf{w}' \circ D\mathbf{x}\|^2 + \lambda \|\mathbf{w} \circ \mathbf{x}\|^2, \quad s.t. \quad \mathbf{A}\mathbf{x} = \mathbf{1} \quad (37)$$

Clearly,  $\mathbf{w}'(\boldsymbol{\omega}) \rightarrow +\infty$  as  $|\boldsymbol{\omega}| \rightarrow +\infty$ , but its behavior near the origin is unclear.

## References

- [1] R. H. Bamberger and M. J. T. Smith, “A filter bank for the directional decomposition of images: theory and design,” *IEEE Transactions on Signal Processing*, vol. 40, no. 4, pp. 882–893, Apr 1992.
- [2] T. T. Nguyen and S. Orintara, “Multiresolution direction filterbanks: theory, design, and applications,” *IEEE Transactions on Signal Processing*, vol. 53, no. 10, pp. 3895–3905, Oct 2005.
- [3] M. N. Do and M. Vetterli, “The contourlet transform: an efficient directional multiresolution image representation,” *Image Processing, IEEE Transactions on*, vol. 14, no. 12, pp. 2091–2106, 2005.
- [4] T. Sauer, “Shearlet multiresolution and multiple refinement.” Kutyniok, Gitta (ed.) et al., *Shearlets. Multiscale analysis for multivariate data*. Boston, MA: Birkhäuser. Applied and Numerical Harmonic Analysis, 199–237 (2012)., 2012.

- [5] G. Easley, D. Labate, and W.-Q. Lim, “Sparse directional image representations using the discrete shearlet transform,” *Applied and Computational Harmonic Analysis*, vol. 25, no. 1, pp. 25–46, 2008.
- [6] E. Candes, L. Demanet, D. Donoho, and L. Ying, “Fast discrete curvelet transforms,” *Multiscale Modeling & Simulation*, vol. 5, no. 3, pp. 861–899, 2006.
- [7] I. W. Selesnick, R. G. Baraniuk, and N. C. Kingsbury, “The dual-tree complex wavelet transform,” *Signal Processing Magazine, IEEE*, vol. 22, no. 6, pp. 123–151, 2005.
- [8] S. Durand, “M-band filtering and nonredundant directional wavelets,” *Applied and Computational Harmonic Analysis*, vol. 22, no. 1, pp. 124 – 139, 2007.
- [9] R. Yin, “Construction of orthonormal directional wavelets based on quincunx dilation subsampling,” in *Sampling Theory and Applications (SampTA), 2015 International Conference on*, May 2015, pp. 292–296.
- [10] A. Cohen and J.-M. Schlenker, “Compactly supported bidimensional wavelet bases with hexagonal symmetry,” *Constructive approximation*, vol. 9, no. 2-3, pp. 209–236, 1993.
- [11] A. Cohen, I. Daubechies, and J.-C. Feauveau, “Biorthogonal bases of compactly supported wavelets,” *Communications on pure and applied mathematics*, vol. 45, no. 5, pp. 485–560, 1992.